Berichte
zur Polar-
und Meeresforschung

641
2012

Reports
on Polar and Marine Research

The Expedition of the Research Vessel "Maria S. Merian" to the South Atlantic in 2011 (MSM 19/2)

Edited by
Gabriele Uenzelmann-Neben
with contributions of the participants

HELMHOLTZ
GEMEINSCHAFT

ALFRED-WEGENER-INSTITUT FÜR
POLAR- UND MEERESFORSCHUNG
in der Helmholtz-Gemeinschaft
D-27570 BREMERHAVEN
Bundesrepublik Deutschland

ISSN 1866-3192

Hinweis

Die Berichte zur Polar- und Meeresforschung werden vom Alfred-Wegener-Institut für Polar- und Meeresforschung in Bremerhaven* in unregelmäßiger Abfolge herausgegeben.

Sie enthalten Beschreibungen und Ergebnisse der vom Institut (AWI) oder mit seiner Unterstützung durchgeführten Forschungsarbeiten in den Polargebieten und in den Meeren.

Es werden veröffentlicht:

- Expeditionsberichte (inkl. Stationslisten und Routenkarten)
- Expeditionsergebnisse (inkl. Dissertationen)
- wissenschaftliche Ergebnisse der Antarktis-Stationen und anderer Forschungs-Stationen des AWI
- Berichte wissenschaftlicher Tagungen

Die Beiträge geben nicht notwendigerweise die Auffassung des Instituts wieder.

Notice

The Reports on Polar and Marine Research are issued by the Alfred Wegener Institute for Polar and Marine Research in Bremerhaven*, Federal Republic of Germany. They are published in irregular intervals.

They contain descriptions and results of scientific activities in polar regions and in the seas either conducted by the Institute (AWI) or with its support.

The following items are published:

- expedition reports (incl. station lists and route maps)
- expedition results (incl. Ph.D. theses)
- scientific results of the Antarctic stations and of other AWI research stations
- reports on scientific meetings

The papers contained in the Reports do not necessarily reflect the opinion of the Institute.

The „Berichte zur Polar- und Meeresforschung” continue the former „Berichte zur Polarforschung”

* Anschrift / Address
Alfred-Wegener-Institut
für Polar- und Meeresforschung
D-27570 Bremerhaven
Germany
www.awi.de

Editor:
Dr. Horst Bornemann

Assistant editor:
Birgit Chiaventone

Die "Berichte zur Polar- und Meeresforschung" (ISSN 1866-3192) werden ab 2008 als Open-Access-Publikation herausgegeben (URL: http://epic-reports.awi.de).

Since 2008 the "Reports on Polar and Marine Research" (ISSN 1866-3192) are available as open-access publications (URL: http://epic-reports.awi.de)

The Expedition of the Research Vessel "Maria S. Merian" to the South Atlantic in 2011 (MSM 19/2)

Edited by
Gabriele Uenzelmann-Neben
with contributions of the participants

Please cite or link this publication using the identifier
hdl:10013/epic.38890 or http://hdl.handle.net/10013/epic.38890

ISSN 1866-3192

Cruise Report
RV MARIA S. MERIAN Cruise MSM19-2

Walvis Bay – Cape Town
23. October – 30. November 2011
Chief Scientist: Gabriele Uenzelmann-Neben
Captain: Karl Friedhelm von Staa

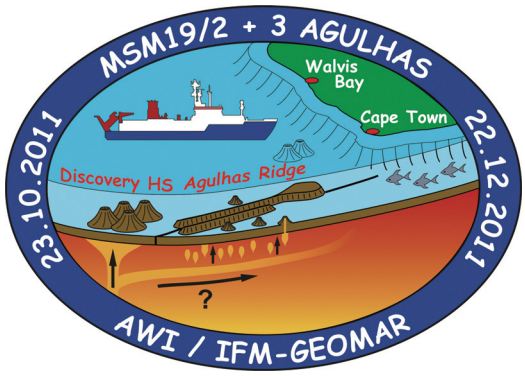

Gabriele Uenzelmann-Neben
Alfred-Wegener- Institut für Polar- und Meeresforschung
Am Alten Hafen 26
D-27558 Bremerhaven

Tel.: +49 471 48311208
Fax: +49 471 48311271
e-mail: Gabriele.Uenzelmann-Neben@awi.de

Contents

Appendices

1. Zusammenfassung / Summary

Der Fahrtabschnitt MSM 19/2 vom 23.10. bis 30.11.2011 mit FS *Maria S. Merian* bestand aus reflexionsseismischen Untersuchungen des Agulhas Rückens, einer topographischen Anomalie der Agulhas-Falkland Fracture Zone im Südatlantik. Der Agulhas Rücken erhebt sich um mehr als 2000 m über den umgebenden Meeresboden und formt so eine Barriere für den Austausch von Wassermassen zwischen hohen und mittleren Breiten. Deformationen der post-oligozänen Sedimente besonders im Kapbecken haben Hinweise darauf ergeben, dass der Agulhas Rücken nach dem Oligozän tektono-magmatisch reaktiviert wurde. Eine detaillierte Erfassung und Analyse der Struktur des Agulhas Rückens und der Kap- und Agulhas Becken mittels seismischer Methoden und ein Anschluß an bestehende ODP Bohrungen (ODP Leg 177) wurde benötigt, um Informationen über die tertiäre Entwicklung des Agulhas Rückens und seinen Einfluß auf die Entwicklung des Pfads des Antarktischen Bodenwassers zu erhalten. Das reflexionsseismische Programm während der Expedition MSM 19/2 wurde derart gestaltet, dass die Struktur des Agulhas Rückens und der Becken bis zum Basement sowie mögliche Sedimentdrifts erfasst wurden. Es wurden insgesamt ~5400 km an hochauflösenden reflexionsseismischen Daten registriert. Parallel zu den seismischen Profilarbeiten wurden bathymetrische und Parasound Messungen durchgeführt. Über die Parasound Registrierungen sind dann signifikante Lokationen für petrologische Beprobungen ausgewählt worden, die während der folgenden Expedition MSM 19/3 durchgeführt werden sollen.
Ergänzt wurden die seismischen Messungen durch 3 CTD Stationen und ADCP Messungen im Gebiet des Agulhas Rückens.

Cruise Leg MSM 19/2 with RV *Maria S. Merian*, leaving Walvis Bay on 23.10., returning to Cape Town on 30.11.2011, comprised seismic reflection studies of the Agulhas Ridge, a topographic anomaly within the Agulhas-Falkland Fracture Zone in the South Atlantic. The Agulhas Ridge rises more than 2000 m above the surrounding seafloor and hence forms an obstacle for the exchange of water masses between high and lower latitudes. A deformation of the post-Oligocene sediments has provided indications for a tectono-magmatic reactivation of the Agulhas Ridge in post-Oligocene times. A detailed study and analysis of the structure of the Agulhas Ridge and the surrounding Cape and Agulhas Basins via seismic data and a correlation with results from ODP Leg 177 Sites 1088, 1089, and 1090 was needed to supply information on the Tertiary development of the Agulhas Ridge and its influence on the path of the Antarctic Bottomwater. Seismic profiles were gathered, which capture the structure of the Agulhas Ridge and the basins down to basement and possible sediment drifts. In total ~5400 km of high resolution seismic reflection data were recorded. Bathymetric and Parasound data were recorded parallel to the seismic profiling. Parasound data were used to pick significant locations for petrological sampling, which will be the focus of the following cruise MSM 19/3.
To complement the seismic and geological studies CTD measurements at 3 locations and ADCP measurements across the whole working area were carried out.

2. Objectives

The Agulhas Ridge forms an elongated part of the Agulhas-Falkland Fracture Zone (AFFZ) (43° S/9° E - 41° S/16° E). It rises more than 2,000 m above the surrounding seafloor. In the northeast the ridge is characterized by a plateau whereas the main ridge is built up by two parallel segments. The ridge segments are separated by a deep depression, which is filled with sediments of > 1000 m thickness. The inner flanks of the ridge segments are much steeper than the outer flanks. The ridge itself is of tectono-magmatic origin and shows only a very thin sedimentary cover. We have aimed to solve the following questions:

1. Has the Agulhas Ridge been reactivated tectono-magmatically? Existing seismic reflection profiles show disturbances in the sedimentary layers. Basement highs in places pierce through the sedimentary column with basement being exposed at the seafloor. At least the pre-Oligocene sequences have been deformed, which points to a reactivation of the ridge in mid-Oligocene times. It is not clear what triggered the reactivation. Material channelized from the Discovery Hotspot via the AAFZ to the Agulhas Ridge has been discussed as an origin (Uenzelmann-Neben and Gohl, 2005). To answer these questions we needed to map the distribution of the sedimentary layers and the spatial extent of the ridge using a grid of seismic reflection profiles and multibeam bathymetric data. This will lead to information on strike and structural relationship of the ridge segments to the AFFZ. Dredge locations were picked for a petrological sampling during MSM 19/3 based on this information.
2. What is the impact of the Agulhas Ridge with respect to oceanic circulation? The Agulhas Ridge has prevented a direct N-S water mass exchange and hence has restricted energy and heat transfer since its formation ~83 Ma. Presently, an eastsetting flow (Antarctic Circumpolar Current ACC, South Atlantic Current SAC, Circumpolar Deepwater CDW) can be observed south of the ridge. North of the ridge a westsetting flow is prevailent. Sediment drifts have been formed parallel to and north of the Agulhas Ridge, which indicate the influence of a water mass similar to CDW starting in Oligocene times. What is the situation between the Agulhas Ridge and the Cape Rise Seamounts? When and with what intensity have water masses started to shape sedimentary deposits there? An expansion of the existing grid of seismic reflection lines (Fig. 2-1) allowed the identification of sediment drifts in the northern Agulhas Basin as well. A detailed analysis will then show similarities in seismic character and the chronological development of drift structures identified north of the Agulhas Ridge.
3. The distribution of sedimentary layers on the eastern plateau of the ridge is largely unknown. This eastern plateau is of major importance, since here the Benguela Current (BC) sets north, the Agulhas Return Current (ARC) has its origin and Agulhas Rings transfer energy and heat from the Indian Ocean. When can we identify the first traces of sediment transport in this area? Can we identify a depth interval for the influence of BC, ARC and Agulhas Rings? The collected grid of seismic reflection profiles will lead to a better understanding on the development of the current systems in this area.

Seismic reflection profile AWI-98007 shows a sedimentary column with at least 1 km thickness on the eastern plateau of the Agulhas Ridge, which are of mid-Miocene to recent age for the upper 240 m. Here, the ridge rises to a water depth of ~1,700 m and hence cannot receive turbidity currents of slides and slump masses. Age, origin and nature of the material are thus unclear. Do the sediments correspond to material observed on the Agulhas Bank or the Falkland Plateau? The newly collected seismic reflection data will enable to map the sedimentary structures and decipher the sedimentation history of the area.

The project comprised geophysical operations in the area of the Agulhas Ridge (Fig. 2.1). Streamer, airguns, as well as PARASOUND and multi-beam systems were used. Seismic reflection profiles were gathered in order to study the sedimentary distribution in relation to the tectonic and oceanographic evolution (yellow lines in Fig. 2.1). Those profiles cover the whole Agulhas Ridge with the transition into the deep sea. Furthermore, the profiles cover the locations of ODP Leg 177 Sites 1088, 1089, and 1090.

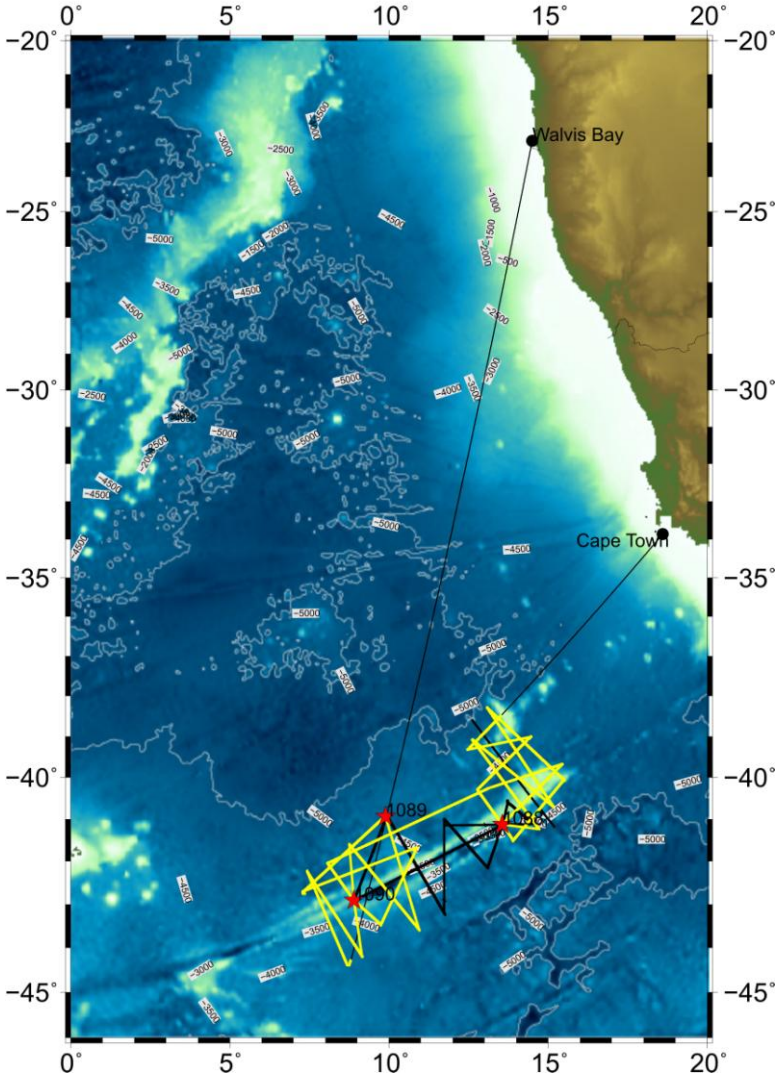

Fig. 2.1: Ship track of RV *Maria S. Merian* cruise MSM19-2 in the South Atlantic with locations of seismic profiles (yellow lines collected during this cruise, black lines collected in 1998) marked. Red stars mark the locations of ODP Leg 177 Sites.

Fig. 2.2: The scientific party of RV *Maria S. Merian* cruise MSM19-2 (**Photo Reinhard Müller).**

3. Cruise Itinerary

(G. Uenzelmann-Neben)

Date	**Approx. Board time (UCT)**	**Programme and event**	**Weather**
23.10.	9:00-19:00	On board, loading, set up of equipment	fine
24.10.	9:00-19:00; 13:00	leave harbour, set up of equipment; start of Parasound and Simrad recording	fine
25.10.		Transit into working area	Increasing winds, high swell
26.10.		Transit to working area	strong winds, high swell
27.10.		Transit to working area	strong winds, high swell
28.10.	 16:30	Transit to working area; CTD/rosette	strong winds, high swell
29.10.	 11:00	Transit to working area; deployment of streamer and airguns; seismic profiling	Strong winds, high swell
30.10.		Seismic profiling	Strong winds, high swell
31.10.		Seismic profiling	Strong winds, high swell
1.11.		Seismic profiling	Strong winds, high swell
2.11.		Seismic profiling	Strong winds, high swell
3.11.		Seismic profiling	Strong winds, high swell
4.11.		Seismic profiling	Strong winds, high swell
5.11.		Seismic profiling	Strong winds, very high swell
6.11.	 21:00	Seismic profiling; retrieval of streamer/airguns due to weather	Strong winds, very high swell
7.11.	 13:00	Bad weather CTD/rosette	Strong winds, very high swell
8.11.	8:00; 11:30	deployment of streamer/airguns; seismic profiling	Strong winds, high swell
9.11.		Seismic profiling	Strong winds, high swell
10.11.		Seismic profiling	Strong winds, high swell
11.11.		Seismic profiling	Strong winds, high swell
12.11.		Seismic profiling	Strong winds, high swell
13.11.		Seismic profiling	Strong winds, high swell
14.11.		Seismic profiling	Strong winds, high swell
15.11.		Seismic profiling	Strong winds, high swell
16.11.		Seismic profiling	Strong winds, high swell
17.11.		Seismic profiling	Strong winds, high swell

18.11.		Seismic profiling	fine
19.11.		Seismic profiling	Medium winds and swell
20.11.		Seismic profiling	Strong winds, high swell
21.11.		Seismic profiling	Strong winds, high swell
22.11.		Seismic profiling	Strong winds, high swell
23.11.		Seismic profiling	Medium winds and swell
24.11.		Seismic profiling	Strong winds, high swell
25.11.		Seismic profiling	Strong winds, high swell
26.11.		Seismic profiling	fine
27.11.	11:00	retrieval of seismic gear; CDT/rosette; leave working area	fine
28.11.		Transit to Cape Town	Medium winds and swell
29.11.	13:00	pilot, back in harbour, towing of containers	Medium winds and swell
30.11.	14:00	Unloading; scientists off-board	fine

4. Geological Background

(G. Uenzelmann-Neben)

4.1 Tectonic development since the break-up of Gondwana

As part of the break-up of Gondwana in the early Cretaceous the 1200 km long Agulhas-Falkland Fracture Zone (AAFZ) developed (Ben Avraham et al., 1997). During opening of the South Atlantic the Falkland Plateau moved along this fracture zone from its initial position south of Africa to its present location (Ben Avraham et al., 1997; LaBrecque and Hayes, 1979; Marks and Tikku, 2001). The inital rifting started north of the AAFZ and east of the Falkland Plateau. A jump of the spreading axis led to formation of an RRR triple junction at anomaly M0 (~109 Ma, late Albian) at the northern end of the present Agulhas Plateau (Ben Avraham et al., 1997; Tucholke et al., 1981). A second jump in spreading axis 83 Ma (chron C34) placed the spreading axis further west in the Agulhas Basin. Another relocation of the spreading axis to the Meteor Rise/Islas Orcadas Rise occurred at 62 Ma (chron 27) (Tucholke et al., 1981; Marks and Stock, 2001).

The Agulhas Ridge forms part of the AAFZ (43°S/9°E - 41°S/16°E) showing an elongated form. It rises more than 2000 m above the surrounding seafloor. The northeastern part of the ridge is characterised by a plateau, while the ridge shows two parallel segments in the southwest (Figs. 4.1 and 5.3). The ridge segments are separated by a deep depression, which is filled with more than 1 km of sediment. The inner flanks of the segments are much steeper than the outside. The ridge itself is of tectono-magmatic origin (Hartnady and le Roex, 1985; Kastens, 1987) and shows only a thin sedimentary cover.

Basement structures disturbing the sedimentary layers have been interpreted to represent a tectono-magmatic reactivation in Oligocene times or younger (Uenzelmann-Neben and Gohl, 2005). The origin of the reactivation is suspected to be material channelized from the Discovery Hotspot west of the Agulhas Ridge.

4.2 Sedimentation and current systems

A reconnaissance survey carried out in the late 1990s provided a first glimps into the sedimentary cover of the Agulhas Ridge. Eight high resolution seismic reflection profiles were correlated with geological information at ODP Leg 177 Sites 1088, 1089, and 1090 (Wildeboer Schut and Uenzelmann-Neben, 2005; Wildeboer Schut and Uenzelmann-Neben, 2006; Wildeboer Schut et al., 2002). Based on this correlation contourite sheets were identified in the southern Cape Basin, which represent an archive of the active bottom currents in this area. The structure of the contouritic sequences indicates a westsetting circulation already in Oligocene times. This direction corresponds to the path of today's Circumpolar Deepwater (CDW). Unfortunately, seismic coverage of the northern Agulhas Basin was sparse. The same is true for the northern Agulhas Ridge. Hence, little is known about the sedimentary sequences in those areas. The northern Agulhas Ridge is of major importance because there CDW, Agulhas Rings and Benguela Current meet and interact. Which effect does this have on sediment transport? Can we reconstruct the development of those three water masses imaging the sedimentary structures?

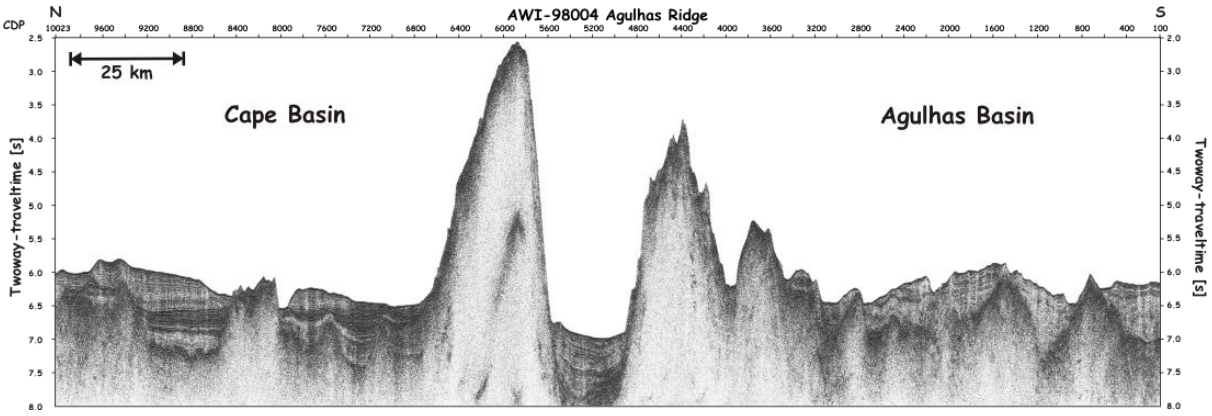

Fig. 4.1: Seismic profile AWI-98004 across the Agulhas Ridge.

4.3 ODP Leg 177 Sites 1088, 1089, and 1090

The seismic profiles connect three ODP sites drilled during Leg 177 (Gersonde et al., 1999). Sites 1088 and 1090 were drilled at the Agulhas Ridge while Site 1089 is located in the adjacent Cape Basin (Fig. 5.3). Middle Miocene to Holocene sediments have been recovered. The core samples were studied with respect to sedimentological, physical and chemical properties and preliminary age models have been established based on combined magneto- and biostratigraphic methods (Gersonde et al., 1999). Site 1088, at 2092 m depth on top of the Agulhas Ridge, consists mainly of calcareous sediments (Shipboard Scientific Party, 1999a), with carbonate percentages varying from 85 to 95 wt.% (Fig. 4.2). In total, 233.7 m of Holocene to Middle Miocene sediments were cored with the objective to recover a long Cenozoic carbonate sequence to study palaeoceanographic changes near the Sub-tropical Front (Shipboard Scientific Party, 1999a). Due to technical problems, it was not possible to drill sediments of early Cenozoic age. Two hiatuses were found, in the Middle Miocene and between Pliocene and Pleistocene. At Site 1089, in the southernmost Cape Basin, a sedimentary sequence of 264.9 m at a water depth of 4620 m was obtained, which documents the Holocene to the Late Pliocene (2.4 Ma) (Fig. 4.2). The Pleistocene section has been deposited at high sedimentation rates (ca. 130–140 m/Ma), while Pliocene sedimentation rates decline to f40 m/Ma (Zielinski and Gersonde, 2002). Core samples between 95 and 156 meters composite depth (mcd) (Shipboard Scientific Party, 1999b) show that the sediments are slightly slumped. However, the sedimentary sequence remains stratigraphically continuous (Zielinski and Gersonde, 2002). This provides records of Pleistocene glaciation cycles with high temporal resolution. The sediments have a fluctuating carbonate content between 0 and 60 wt.% due to variation in the amounts of terrigenous mud and changes in carbonate preservation. The Pliocene/Pleistocene boundary is well defined in Site 1089 and is located at ca. 230 mcd (Zielinski and Gersonde, 2002).

Site 1090, at the southern end of the Agulhas Ridge, was placed at a water depth of 3702 m. Due to one or two disconformities between 71.5 and 78.5 mcd, which separate lower Pliocene and probably uppermost Miocene sediments from lower Miocene sequences, drilling at Site 1090 reached the Middle Eocene at 397 meters below sea floor (mbsf) (Shipboard Scientific Party, 1999c). While the study of planktic foraminifers by (Galeotti et

al., 2002) indicates two disconformities at 71.5 and 78.5 mcd, separating Early Pliocene from Late Miocene and Late Miocene from Early Miocene, respectively, shipboard stratigraphic data also including the geomagnetic inclination record reveal one disconformity at around 70 mcd which separates the Early Pliocene from the Early Miocene and spans ca. 14 Ma (Shipboard Scientific Party, 1999c). Increased bottom-current velocity caused widespread hiatuses in oceanic sediments in many other areas as well (e.g. Keller, 1987; Ledbetter and Ciesielski, 1982). The study of planktic foraminifers also indicates strong reworking of late Cretaceous (Campanian–Maastrichtian to Miocene) planktic foraminifers at around 71.5 mcd (Galeotti et al., 2002). Three other short-ranging disconformities have been encountered in the Pleistocene (Venz and Hodell, 2002), two being close to the Plio/Pleistocene boundary at around 40–43 mcd. Calcareous nannofossil investigations point to a hiatus at around 220 mcd, in the Early Oligocene, which spans about 3 Ma (Marino and Flores, 2002). Nannofossils, diatoms and mud comprise the major lithologic components of the sediments recovered at Site 1090. While the Middle and early Late Eocene consist of mud-bearing nannofossil ooze and chalk, the Late Eocene to Early Miocene is characterised by mudbearing diatom ooze and diatom bearing nannofossil ooze and chalk. The Plio/Pleistocene sequences are characterised by alternations of nannofossil ooze and diatom-bearing nannofossil ooze. A chert layer has been encountered at 290 and 340 mbsf, respectively, in the Eocene section (Shipboard Scientific Party, 1999c). The disconformity at around 70 mcd is underlain by a tephra layer (Shipboard Scientific Party, 1999c).

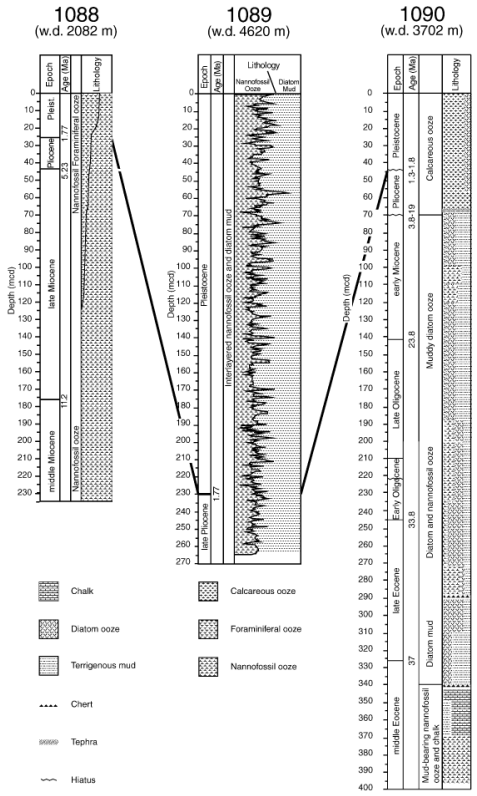

Fig. 4.2: Lithology of ODP Leg 177 Sites 1088, 1089, and 1090 (Gersonde et al., 1999; Shipboard Scientific Party, 1999a; Shipboard Scientific Party, 1999b; Shipboard Scientific Party, 1999c).

5. Scientific Programmes - Preliminary Results

5.1 Seismic reflection profiling

(G. Uenzelmann-Neben, H. Cawthra, Th. Eggers, J. Grützner, M. Horn, A. Müller-Michaelis, D. Penshorn, E. Seidel, S. Suckro)

5.1.1 Methods

The application of seismic methods was the primary operational objective of MSM 19/2 in order to obtain information on the sedimentary distribution in the area of the Agulhas Ridge. We used a standard multi-channel seismic reflection technique to image the outline and reflectivity characteristics of the sedimentary layers and the structure of the sub-sedimentary basement and lower crust by recording the returning near-vertical wave field. Figure 5.1 illustrates the principles of this technique.

5.1.2 Seismic equipment

5.1.2.1 Seismic sources, triggering and timing

We used a cluster of 4 GI-guns to resolve the sedimentary layers. A single GI-Gun™ is made of two independent airguns within the same body. The first airgun ("Generator") produces the primary pulse, while the second airgun ("Injector") is used to control the oscillation of the bubble produced by the "Generator". We used the "Generator" with a volume of 0.72 litres (45 in^3) and fired the "Injector" (1.68 litres = 105 in^3) with a delay of 33 ms. This leads to an almost bubble-free signal. The guns were towed 30 m behind the vessel in 2 m depth and fired every 10 s (~25 m shot interval).

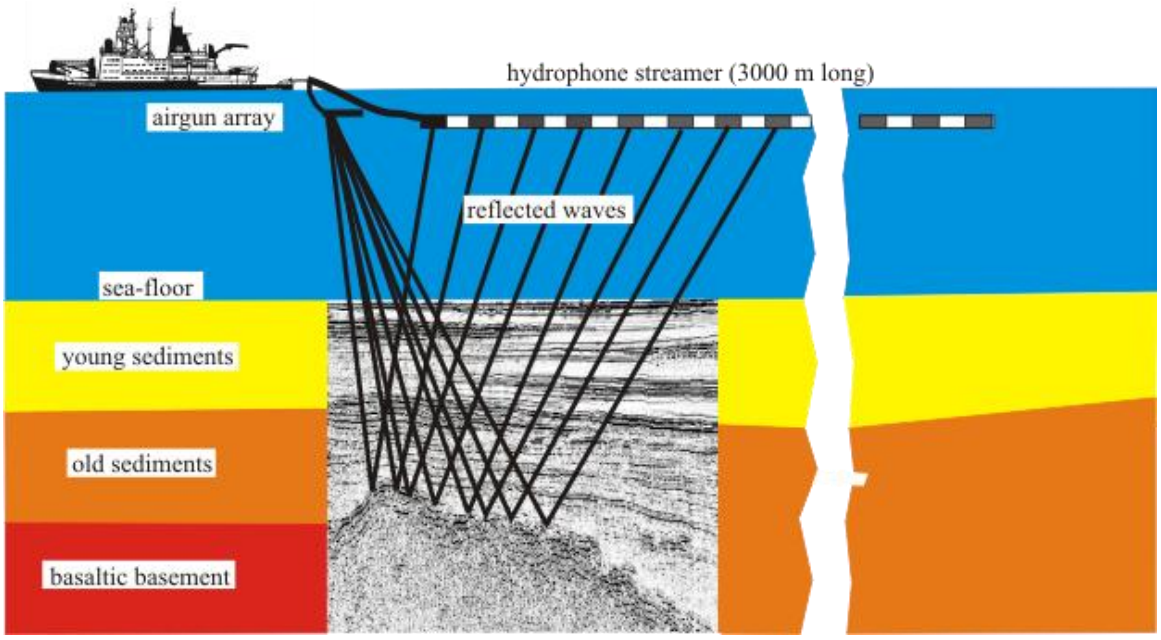

Fig. 5.1: Principle of marine seismic reflection surveying.

Seismic data acquisition requires a very precise timing system, because seismic sources and recordings systems must by synchronised. A combined electric trigger-clock system was in operation in order (1) to provide the firing signal for the electric airgun valves, and (2) to provide the time-control of the seismic data recording. Due to the variable time difference in

the NMEA format of the ship-provided clock and the DVS system, a separate Meinberg GPS clock was used with an antenna mounted on the upper deck. The clock provides UTC date and time (minute and second) pulses. Airguns were fired with gradually increasing working pressure (ramping up) at the beginning of a profile and after shot interruptions.

5.1.2.2 Multi-channel reflection recording system

For multi-channel reflection data acquisition, a complete digital seismic streamer and recording system was used. The system consists of a large capacity, fully integrated, high resolution marine seismic data acquisition system (SERCEL SEAL™) which is composed of both onboard and in-sea equipment (Fig. 5.2). The streamer is a 240-channel hydrophone array which is coupled to the onboard recorder via a fibre-optic tow leader and a deck lead. The data collected by the hydrophone array is firstly converted from an analogue signal to digital via an A/D converter and then converted to a 24-bit complement format at 0.25 ms sample rate by a DSP. The data is routed to a Line Acquisition Unit Marine (LAUM) at this point, one of these being located every five Acquisition Line Sections or 750 m. The LAUM decimates, filters and compresses the data before routing them through the tow leader and deck lead to the on-board equipment.

Fig. 5.2: SERCEL SEAL™ digital multichannel seismic system and the recordings units.

The coupling of the streamer with the Control Module (CMXL) is made via the Deck Cable Crossing Unit (DCXU) which also acts as a LAUM for the first 60 channels of the streamer. The CMXL decompresses, demultiplexes and then performs IEEE 32-bit conversion to the data. The data are collected via a network switch and converted to SEGD

by the PRM, the PRM being a processor software module used for formatting data to and from the cartridge drives, the plotters and Seapro QC™.

All system parameters can be set through the Human Computer Interface (HCI) which displays the systems activity such as print parameters, log files, high resolution graphic display and test results.

Cable depth keeping was monitored on Digicourse™ software, and adjustment to depths was made with Digibirds™, Model 5010. The Digicourse™ software gives a continuously updated graphical display of depths and wing angles via the Digibirds™ which are situated at 300 m intervals along the streamer.

Table 5.1: Specification of SEAL system

Acquisition Line Section Spec.	
Length	150 m
Channels	12
Phones/group	16
Group length	12.5 m
Sensitivity	20 V/Bar open ended
Capacity	256 μf

The data were recorded with the following parameters (also Appendix 5):

Table 5.2: Brief description of seismic recording parameters

Profile Name	*Active Length*	*Lead-in*	*Record Length*	*Sample Rate*
AWI-20110401	3000 m	191 m	9 s	1 ms
AWI-20110402	3000 m	191 m	9 s	1 ms
AWI-20110403	3000 m	191 m	9 s	1 ms
AWI-20110404	3000 m	191 m	9 s	1 ms
AWI-20110405	3000 m	191 m	9 s	1 ms
AWI-20110406	3000 m	191 m	9 s	1 ms
AWI-20110407	3000 m	191 m	9 s	1 ms
AWI-20110408	3000 m	191 m	9 s	1 ms
AWI-20110409	3000 m	191 m	9 s	1 ms
AWI-20110410	3000 m	191 m	9 s	1 ms
AWI-20110411	3000 m	191 m	9 s	1 ms
AWI-20110412	3000 m	191 m	9 s	1 ms
AWI-20110413	3000 m	191 m	9 s	1 ms
AWI-20110414	3000 m	191 m	9 s	1 ms
AWI-20110415	3000 m	191 m	9 s	1 ms
AWI-20110416	3000 m	191 m	9 s	1 ms

AWI-20110417	3000 m	191 m	9 s	1 ms
AWI-20110418	3000 m	191 m	9 s	1 ms
AWI-20110419	3000 m	191 m	9 s	1 ms
AWI-20110420	3000 m	191 m	9 s	1 ms
AWI-20110421	3000 m	191 m	9 s	1 ms

.

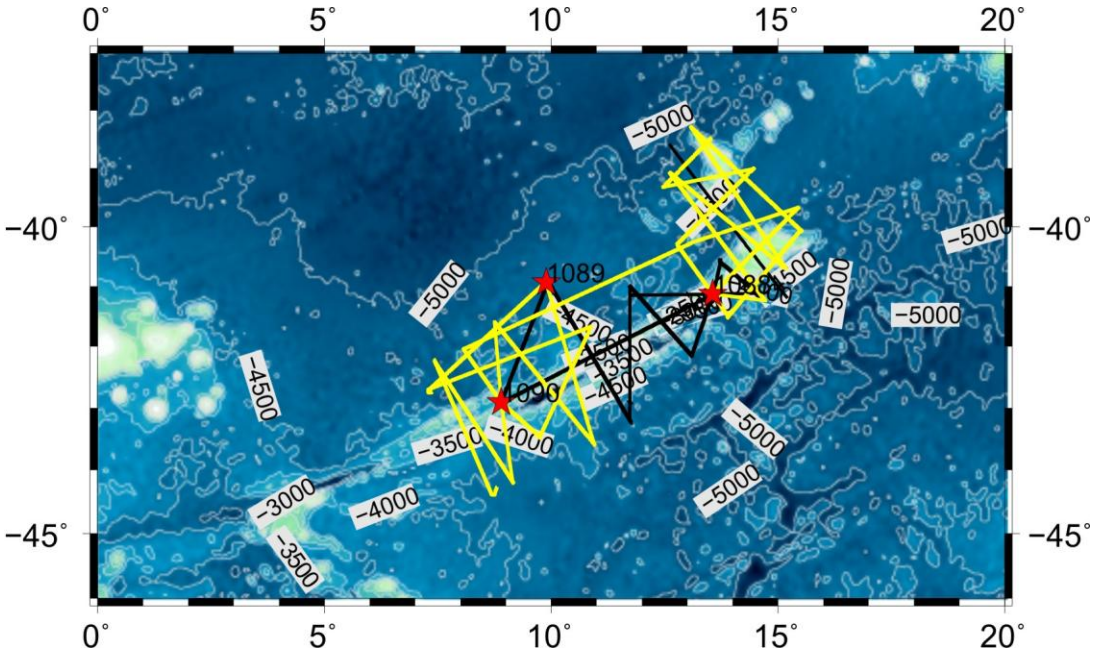

Fig. 5.3: Bathymetric map of the Agulhas Ridge with locations of the newly collected seismic lines in yellow. Black lines show the locations of seismic lines collected in 1998. Red stars show the locations of ODP Leg 177 Sites 1088, 1089, and 1090.

5.1.3 Preliminary Results

As detailed seismic processing is time-consuming and could not be carried out on board, only a first, preliminary interpretation could be performed on board during the cruise.

The seismic profiles were concentrated on the northeastern and the southwestern part of the Agulhas Ridge (Fig. 5.3). The area in between those two parts was already surveyed in 1998. A long seismic line connects both areas. The seismic lines cross the ridge from the Cape Basin in the north to the Agulhas Basin in the south. Three sites drilled during ODP Leg 177 (1088, 1089, and 1090, (Gersonde et al., 1999)) were crossed several times to allow a correlation of the seismic data with geological information.

The Agulhas Ridge itself consists of up to four parallel segments in the south, which are separated by depressions. Those depressions are filled with up to 1 s TWT sediments. In the north, the ridge is characterised by a plateau. Sediment thickness on this plateau is up to 1.5 km. There, the sedimentary sequences are well layered. In places, strong erosion and a wedge-out of sequences at the seafloor can be observed indicating erosion due to current activity. The basement shows several vertical displacements pointing towards tectonic

activity. We further observe a number of seamounts on the plateau. The flank of the ridge down into the Agulhas Basin is very steep. The flank into the Cape Basin is characterised by several faults.

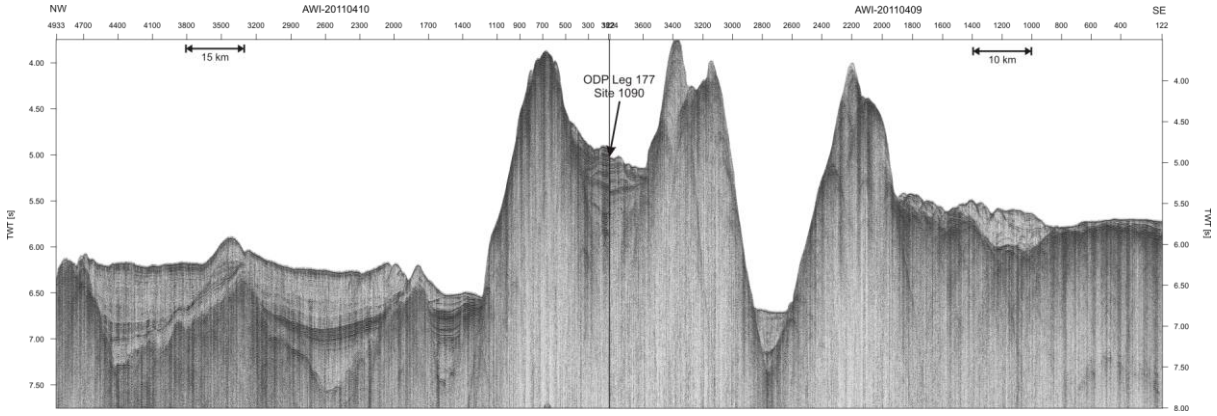

Fig. 5.4: Lines AWI-201104009/10 across the Agulhas Ridge showing the location of ODP Leg 177 Site 1090.

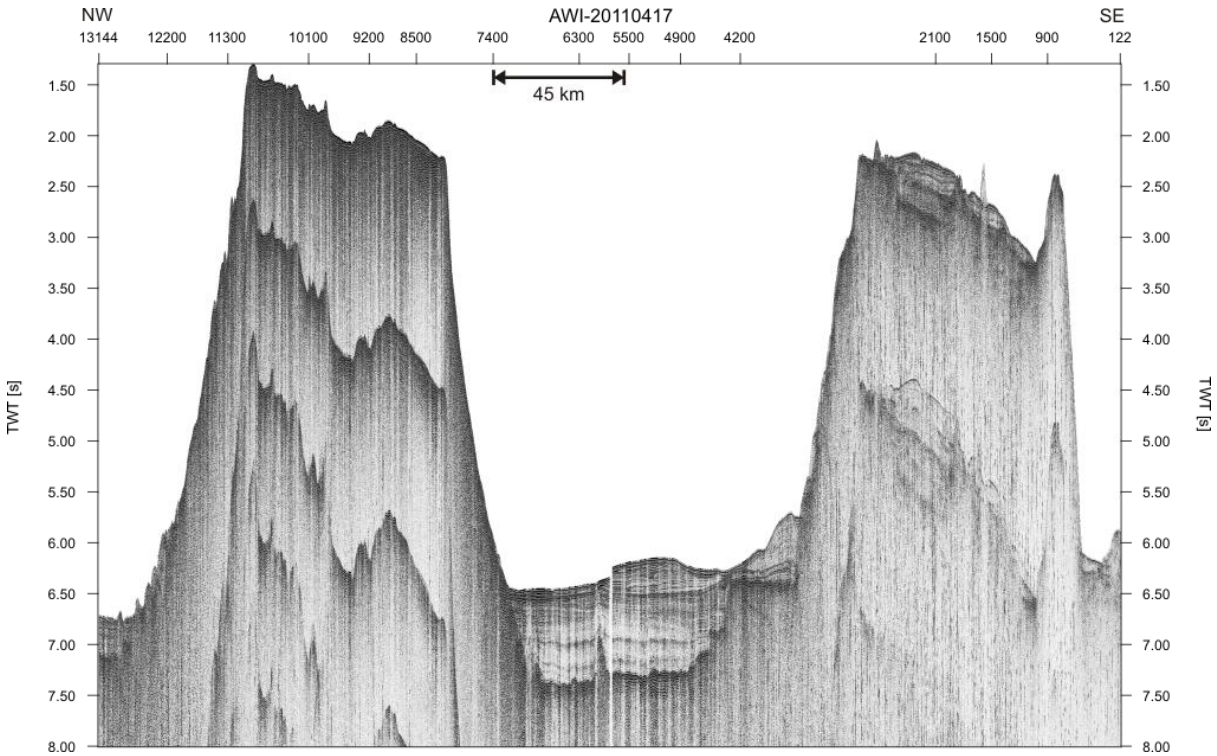

Fig. 5.5: Line AWI-20110417 showing a cross section from the plateau of the Agulhas Ridge via the Cape Basin to the Cape Rise Seamount.

Basement in the Cape Basin is characterised by a large number of highs as well as seamounts, which disturb the older sedimentary sequences and are indicative of a tectono-magmatic reactivation. Sediment drifts and moats can be observed in the vicinity of those basement highs (Figs. 5.4 and 5.5). In contrast to this general appearance the basement is quite smooth towards the Cape Rise Seamount (Fig. 5.5). There we also observe rough

basement without a significant sedimentary cover as well as strong erosion. West of the Cape Rise Seamount we observe two further seamounts separated by a small depression with a sediment filling of 250 ms thickness. The Cape Rise Seamount itself shows a flat top without a significant sediment cover. Northeast of the Cape Rise Seamount we observe another well developed sediment drift. In general, drift formation appears to have commenced after deposition of a pronounced reflector band, which Wildeboer Schut et al. (2005) identified as Oligocene.

For the Agulhas Basin south of the Agulhas Ridge we could identify a large number of extended sediment drifts. A moat separates the sediment drifts from the southern flank of the Agulhas Ridge (Fig. 5.4). Several phases of drift formation and current modifications can be distinguished via a relocation of the drift apex. Basement highs, which in parts form wide blocks, appear quite regularly in the Agulhas Basin indicating tectonic movements.

5.2 Swath Bathymetry (SIMRAD)

(T. Dufek)

5.2.1 Introduction

Swath sonar systems are used for seafloor mapping. They calculate the water depth by runtime measurement of an acoustic signal, which is transmitted and received by the transducer mounted in the ship's hull. Therefore information of the water sound velocity is very important to obtain bathymetric data in high quality.

Bathymetric mapping was conducted throughout the cruise MSM19/2 with the echo sounder system SIMRAD EM120 (12 kHz). The data was used to provide the scientists on board with precise depth information and bathymetric charts of the research area. The data provided also important information for the following cruise MSM19/3 when it was consulted for project planning. Furthermore the collected data will be contributed to the global bathymetric dataset GEBCO (The General Bathymetric Chart of the Ocean) for further improvement of the global dataset.

5.2.2 Technical Aspects and Mode of Operation

The bathymetric swath system mounted onboard RV *Maria S. Merian* consists of the following components:

Multibeam Echosounder:	Kongsberg Simrad EM120 (12 kHz)
Beam steering sound velocity probe:	AML SV Probe
Motion compensation:	Kongsberg Seatex SeaPath 200
Heading/gyro sensor:	Kongsberg Seatex SeaPath 200
Positioning	Primary antenna of Kongsberg Seatex SeaPath 200

The multibeam echo sounder SIMRAD EM120 (Kongsberg) transmits 191 beams per ping with a 2° angle across and along-track. The operating frequency of the system is 12 kHz. The angular coverage sector can be set up to 150° (75° each side). During the cruise MSM 19/2 the angular coverage sector was adjusted according to the weather conditions and data quality. The aperture angle varied between 130° during regular sea conditions and 100°

during rougher weather conditions when a high noise level was observed in the acquired data. The beam spacing method was set to be equidistant throughout the cruise.

5.3.3 Preliminary results

Bathymetric mapping was conducted throughout the cruise. The system was turned on the 24th October 2011 at 18:00 (UTC) in the Namibian EEZ and turned off on the 28th November 2011 at 6:00 (UTC) before entering the South African EEZ. The system was monitored during data acquisition to ensure high resolution measurements and avoid larger data losses. A decrease in data quality was observed in connection to strong roll motion (>10°) of the vessel, when the ship's heading was roughly perpendicular to the orientation of the swell. Only every fifth measurement could then be partly used. Similar observations were made in the PARASOUND data. For a more detailed description and a discussion of the possible causes see Chapter 5.3 Marine Sediment Echosounding using PARASOUND. In Figure 5.6 the course dependent difference in data quality is shown.

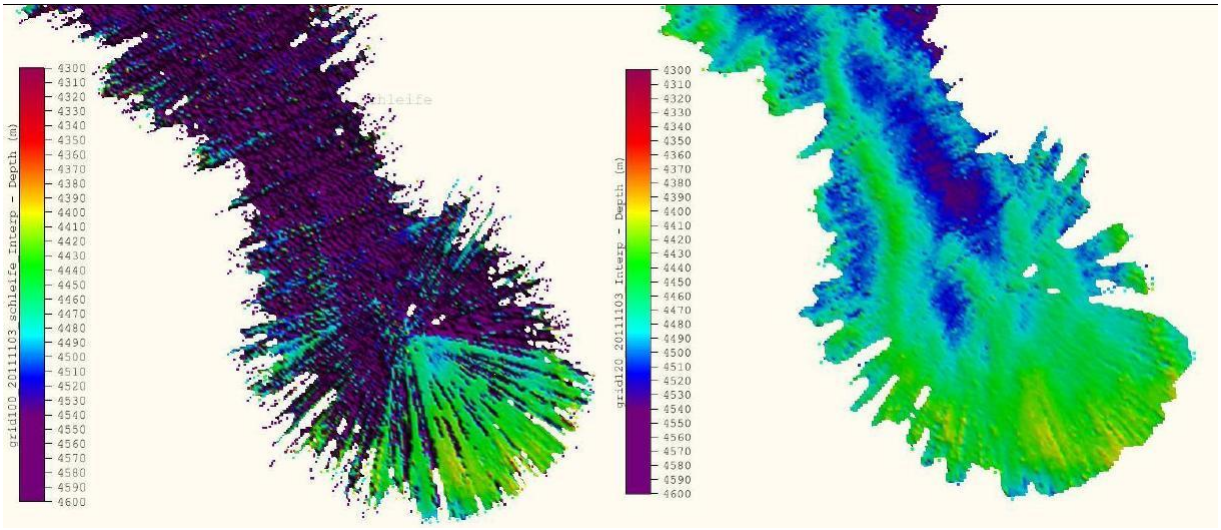

Fig. 5.6: Left: Bad quality raw bathymetric data in bad quality. During the turn onto an adjacent line when the course changes the increase in quality (decrease in noise) is clearly visible. Right: The same bathymetric dataset after editing. Seafloor topography can now be clearly seen.

The outer beams occasionally failed, but after a complete restart of the system they were working properly in most cases. A total of three restarts of the EM120 were necessary during the cruise due to missing outer beams.

5.2.4 Water Sound Velocity Profiles

Three CTD (Conductivity, Temperature, Depth) casts were carried out during the cruise. Two were taken in the western part of the main research area and one in the eastern part (see Chapter 5.4 CTD). The CTD casts provided water sound velocity profiles, which were entered into the SIMRAD EM120 system to ensure high quality measurements. Information of the water sound velocity of the upper metres of the water column were acquired by the AML sound velocity probe and used during bathymetric data acquisition.

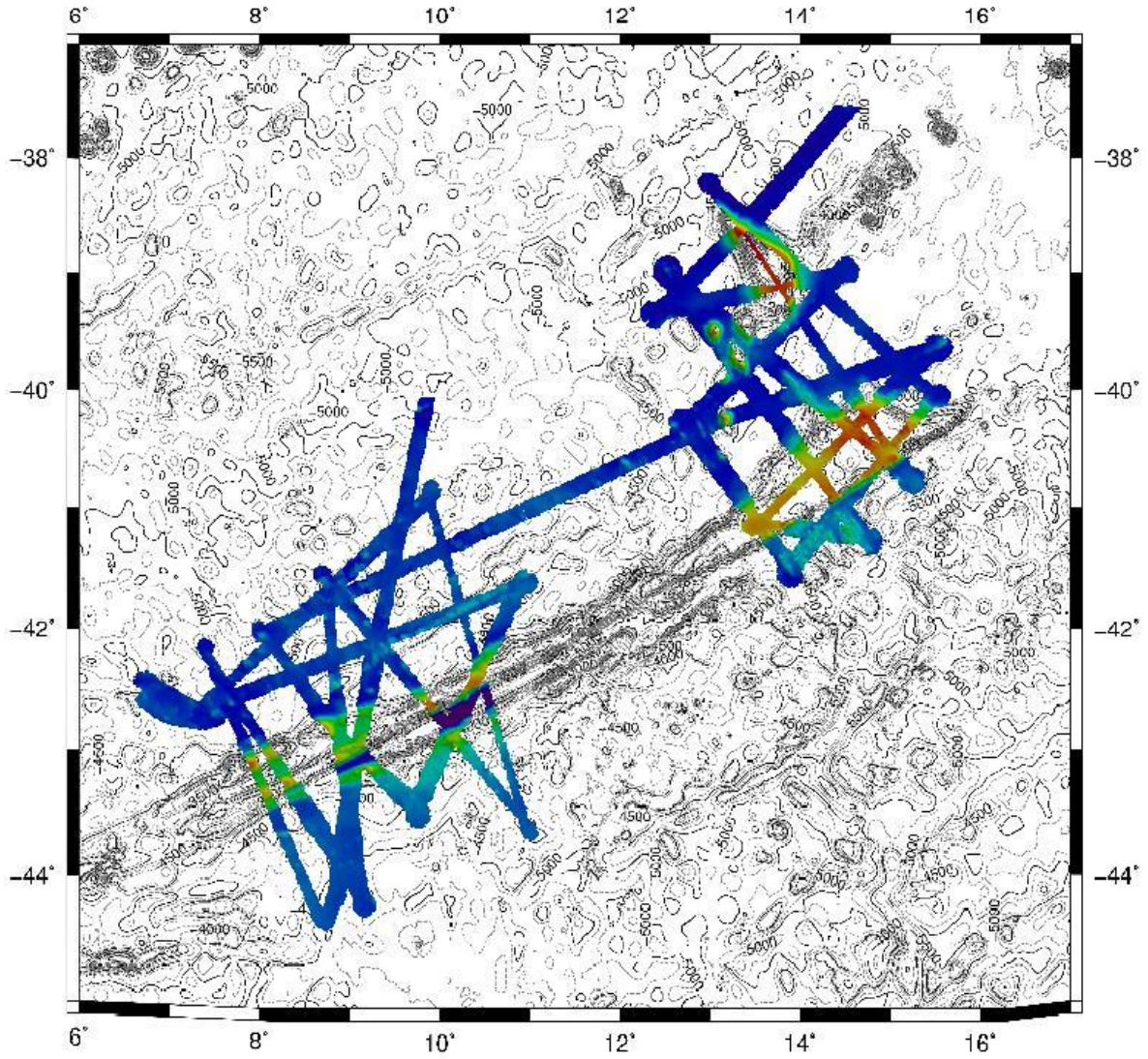

Fig. 5.7: An overview of the bathymetric data collected in the Agulhas Ridge study area.

When the eastern part of the research area was approached on the 13th of November, a strong increase of around 7° C (from 11° C to 18° C) in the temperature of the water surface was observed. The increased temperature held on until the system was turned off on the 28th of November. The resulting change in water sound velocity in the upper metres of the water column was around 25 m/s.

5.2.5 Data Processing

Data files of 30 min duration were recorded in SIMRAD *.all-format using the Kongsberg data acquisition software SIS. These files were imported into the post processing software CARIS HIPS & SIPS 6.1. The data was checked manually for navigation errors and gross blunders in depth measurements.

Grids (BASE Surfaces) were created from the processed data using CARIS HIPS & SIPS 6.1. These were used for checking the quality of the processed data and visualization. The data was also exported in ascii format for map generation using the open-source software GMT (Generic Mapping Tool).

In Figure 5.7 a plot of the collected data in the research area of the Agulhas Ridge is shown.

5.3. Marine Sediment Echosounding using PARASOUND

(F. Niessen)

5.3.1 Scientific Objectives

Bottom and sub-bottom reflection patterns obtained by PARASOUND characterize the uppermost sediments of the ocean in terms of their acoustic behavior down to about 200 m below the sea floor. This can be used to study depositional environments and their variation in space and time. The objectives of sediment echosounding during MSM 19/2 were:

- to provide the data base for an acoustic facies interpretation of the upper 200 m of sediments which are predominantly drift deposits indicative for different bottom water currents and their spatial and temporal variability, and, thereby,
- to provide a high-resolution counterpart for the uppermost sections of seismic profiles recorded during the cruise,
- to directly correlate physical property data of ODP sites 1088-1090 to PARASOUND profiles recorded across the coring locations,
- to obtain different pattern of high-resolution acoustic stratigraphy useful for lateral correlation over shorter and longer distances thereby aiding the transfer of ODP core stratigraphy into the different drift deposits,
- to provide information about the sediment cover on top of ridge and seamount peaks in order to support selection of potential stations for petrographical sampling in the same area of investigation during the forthcoming leg MSM-19/3.

5.3.2 Technical Aspects and Modes of Operation

RV *Maria S. Merian* is equipped with a Deep Sea Sediment Echo Sounder PARASOUND (ATLAS HYDROGRAPHIC, Bremen, Germany) DS III-P70 similar to the systems installed on other German RVs such as *Polarstern*, *Meteor* and *Sonne*. An overview about the system set up and operation of "PARASOUND DS III-P70" is given by Niessen et al. (in Klages and Thiede, 2010) and Niessen et al. (in Schiel, 2009).

The hull-mounted PARASOUND system generates two primary frequencies selectable between 18 and 23.5 kHz transmitting in a narrow beam of 4° at high power. As a result of the non-linear acoustic behavior of water, the so-called "Parametric Effect", two secondary harmonic frequencies are generated of which one is the difference (e.g. 4 kHz) and the other the sum (e.g. 40 kHz) of the two primary frequencies, respectively. As a result of the longer wave length, the lower parametric frequency allows sub-bottom penetration up to 200 m (depending on sediment conditions) with a vertical resolution of about 0.30 m. The primary advantage of parametric echosounders is based on the fact that the sediment-penetrating pulse is generated within the narrow beam of the primary frequencies thereby providing a very high lateral resolution compared to conventional 4 kHz-systems.

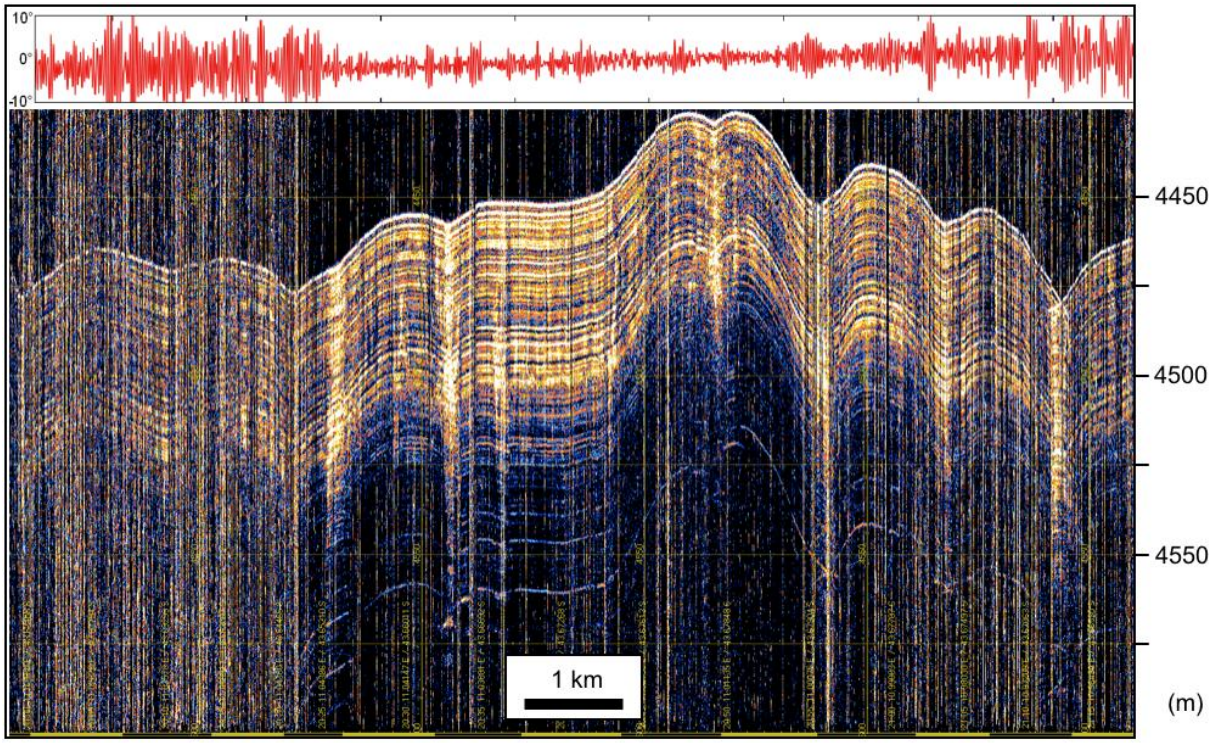

Fig. 5.8: PARASOUND profile recorded in the turning loop between seismic profiles AWI-20110404 and 0405 (3.11.2011, 19:55 to 21:35 UTC). Data quality (signal to noise ratio) is compared to ship motion (rolling angles of +10° to -10° plotted in red at the upper end of the figure). Plot produced using ATLAS PARASTORE-3 software.

Table 5.3: Settings of PARASOUND operation used on MSM-19/2

Used Settings	**Selected Options**	**Selected Ranges**
Mode of Operation	P-SBP/SBES	PHF, (SHF), SLF
Frequency	PHF SHF SLF	18.072 kHz (41.66 kHz) until 21.10. 07:26 UTC 4.016 kHz
Pulselength	No. of Periods Length	2 (normal operation) up to 16 (demand) 0.5 ms at 2 periods
Transmission Source Level	Transmission Power Transmission Voltage	100% 159 V
Beam Steering	none	
Mode of Transmisson	Single Pulse Quasi-Equidistant	 Interval 400-2490 ms
Pulse Type	Continuous Wave	
Pulse Shape	Rectangular	
Receiver Band Width	Output Sample Rate (OSR) Band Width (% of OSR)	6.1, 12.2 kHz (automatic mode) 66%, 33% (automatic mode)
Reception Shading	none	
System Depth Source	Fix Min/Max Depth Limit	Manual (>95% of operation) Other (EM-120) Controlled Atlas PHF

		Atlas Parastore
Water Velocity	C-Mean C-Keel	Manual 1500 m/s Manual 1500 m/s
Data Recording	PHF SLF	Full Profile Full Profile

On RV *Maria S. Merian*, PARASOUND DS III-P70 is controlled by two operator software packages plus server software running in the background. These processes are running simultaneously on a PC under "Windows XP". (i) ATLAS HYDROMAP CONTROL is used to run the system by an operator. The selected modes of operation, sounding options and ranges used during the cruise are summarized in Table 5.3. A list of abbreviations is given at the end of this chapter. (ii) ATLAS PARASTORE-3 is used by the operator for on-line visualization (processing) of received data on PC screen, for data storage and printing. It can also be used for replaying of recorded data, post-processing and further data storage in different output formats (PS3 and/or SEG-Y). For any further details the reader is referred to the operator manuals of ATLAS HYDROMAP CONTROL, of ATLAS PARASTORE-3 and some basic descriptions given by Niessen et al. (in Schiel, 2009).

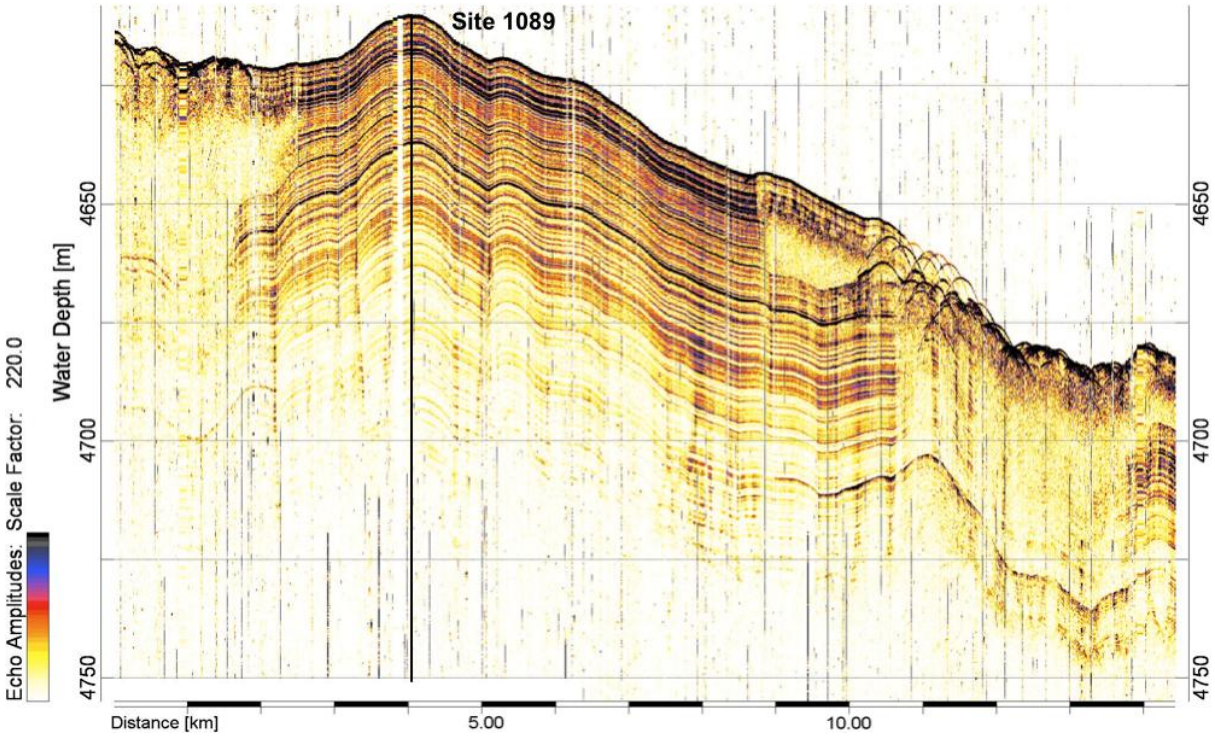

Fig. 5.9: PARASOUND profile recorded on seismic line AWI-20110406 (5.11.2011, 10:00 – 11:30 UTC) with location of ODP site 1089 (Leg 177). Plot produced using SeNT software.

5.3.3 Data Acquisition, Management, System Failure and Data Quality

During MS-19/2 digital data acquisition and storage were switched on with full data acquisition, when the 12 nm zone of the State of Namibia was left on October 24 at 16:19

UTC. Acquisition and storage of data were finished after a final Operator-PC crash on November 28 at 03:49 UTC after the working area was left but before entering the 200 nm EEZ of the State of South Africa. PARASOUND was continuously operating during the period stated above unless acquisition was interrupted by system crashes or switched to standby on stations (Tab. 5.4). Acquisition included PHF and SLF data whenever the system was running. In addition, during the first few days of the expedition, SHF data were acquired and stored. The reflected SHF signal from the sea floor became hardly visible below about 1500 m of water depth and the record appeared very noisy. Thus, at 23:58 UTC on October 28 the last SHF file was stored to disc and SHF acquisition terminated. Both acquisition of PHF and SLF continued and traces were visualized as online profiles on screen. SLF profiles (200 m depth windows) and online status (in 120 s intervals) were printed on A4 pages.

For the periods defined above nine different types of on-line data files were stored on hard discs:

(1-3) PHF data in ASD, PS3 and SEG-Y formats,
(4-6) SLF data in ASD, PS3 and SEG-Y formats,
(7) SHF data in ASD format,
(8) Navigation data and general PARASOUND settings (120 s or 60 s intervals) in ASCII format (not complete),
(9) Auxiliary data about ATLAS PARASTORE 3 settings in ASCII format (not complete).

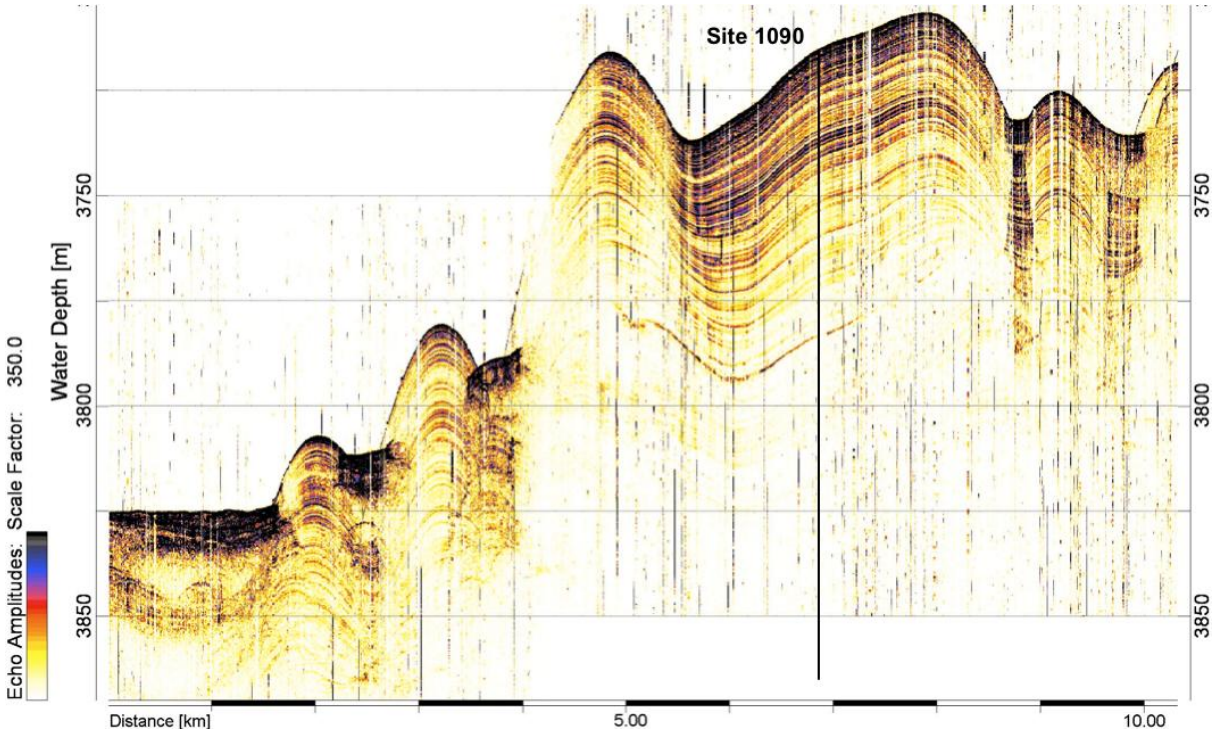

Fig. 5.10: PARASOUND profile recorded on seismic lines AWI-20110409 and -20110410 (11.11.2011, 11:11-12:20 UTC) with location of ODP Site 1090 (ODP Leg 177) as the boundary between the two seismic lines. Plot produced using SeNT software.

All ASD data files stored are automatically packed into "cabinet files" by Atlas software. The files are named according to date and time of recording (containing about 10 minutes of acquired data per file). The data have been sorted by the operator into folders according to data type and recording dates (0 to 24 hours UTC), copied to one external hard disk via fast USB-board and backed up on a second hard disc. In total 39358 files in 239 folders of data with a total volume of 333 GB were stored on external discs. These data will be transferred to the AWI data base for being available through PANGAEA (www.pangaea.de) after publication. We will use the ship's database (full record of GPS-positions in one-minute intervals) for geo-referencing the PARASOUND data of the cruise.
During the entire period of acquisition the system was operator controlled (watch keeping). Book keeping was carried out including basic PARASOUND system settings, some navigation information, various kinds of remarks as well as a low-resolution bathymetry plot with hand-drawn sub-bottom sediment structures. Time windows with data of specific interest (e.g. ODP sites or characteristic examples from the working area) were selected and replayed during the cruise using optimal settings of ATLAS PARASTORE-3 and SeNT (Hanno Keil, MARUM, University of Bremen).

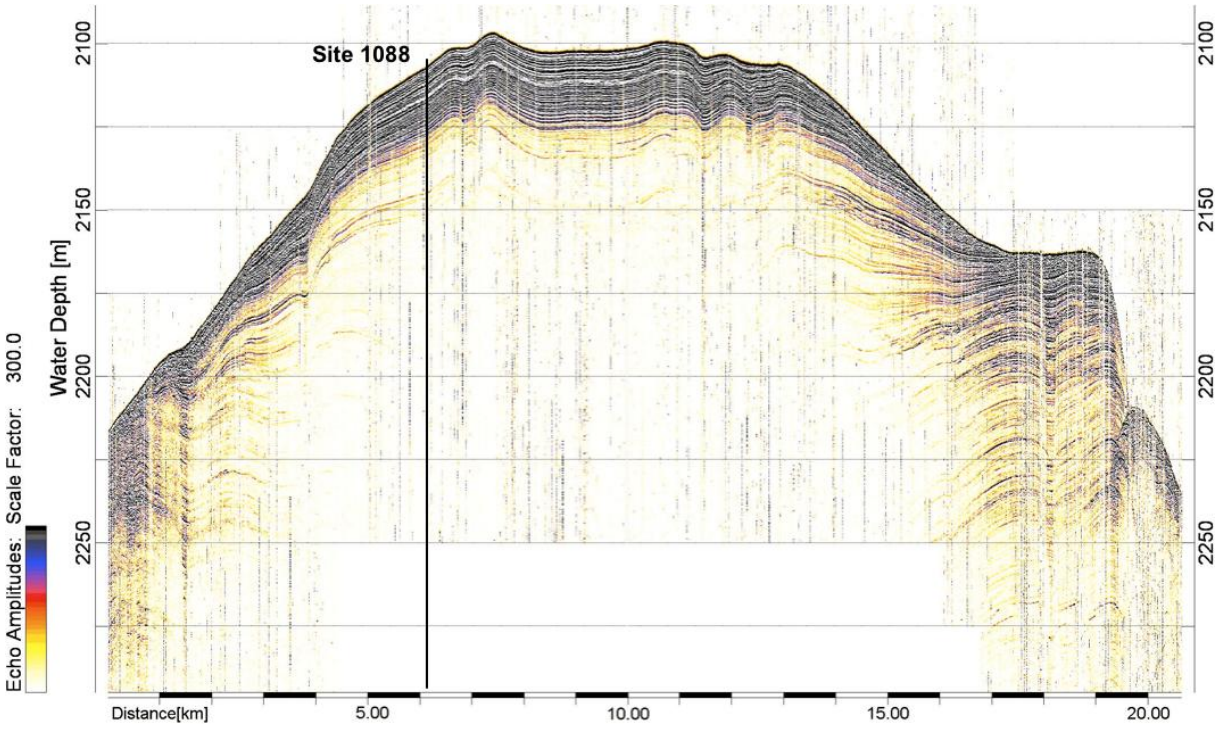

Fig. 5.11: PARASOUND profile recorded on seismic line AWI-20110413 (16.11.2011, 06:45 – 09:00 UTC) with location of ODP Site 1088 (ODP Leg 177). Plot produced using SeNT software (negative flanks suppressed).

In total a number of 13 Operator PC or system crashes were observed during the cruise. These crashes were caused by failures of WINDOWS-XP, ATLAS HYDROMAP CONTROL, ATLAS PARASTORE-3, CM and/or SPM as well as the LAN Router (Tab. 5.4). The loss of data is summarized (Table 5.4). In total a period of 17.93 hours of data acquisition was lost, which is equivalent to 1.6 % of the total time of PARASOUND

operation, where profiling in the area under investigation was carried out (station time not included, Tab. 5.4). In addition, until November 11 we have noted a total of 146 CM-recoveries, after which the system returned to normal operation automatically. After November 11, the record of CM recoveries is fragmental because the CM-message window of ATLAS HYDROMAP CONTROL failed due to a network or data exchange problem. However, when noted hints of CM recoveries were added to the record (Tab. 5.4). CM recoveries caused small losses of data (about 0.6% of the total operation time) as each time acquisition interrupted for periods between 30 seconds and 2 minutes (Tab. 5.4).

Table 5.4: Summary of time windows when PARASOUND data acquisition was not possible due to system failure and repair and the system was on standby during stations

date 2011	**From UTC**	**Until UTC**	**duration (h)**	**reason**
25.10	8:45	23:31	0.22	13 times CM-Recovery-Action
26.10.	2:03	5:45	0.05	3 times CM-Recovery-Action
	8:23	8:39	0.27	Disconnect and restart PC, PC very slow, no copy of data possible, no task manager
30.10	5:45	8:57	3.2	Parastore Windows stuck restart after Atlas Parastore, scan for virus (one found)
	12:36	23:03	0.13	8 times CM-Recovery-Action
31.10.	3:36	23:04	0.22	13 times CM-Recovery-Action
01.11.	3:38	23:33	0.18	11 times CM-Recovery-Action
	21:15	22:15	1.0	System crash, unable to transfer PHF/SLF data from CM, restart
02.11.	0:35	22:25	0.18	11 times CM-Recovery-Action
03.11.	0:56	20:35	0.23	14 times CM-Recovery-Action
	2:37	2:38	0.02	No data without error message
04.11.	0:20	22:18	0.33	20 times CM-Recovery-Action
05.11.	1:09	21:35	0.33	20 times CM-Recovery-Action
06.11.	6:05	11:57	0.07	4 times CM-Recovery-Action
	11:57	12:20	0.38	CM-Recovery Restart, Driver P70 is not sending telegramms, Transmission Stop, CM-crash and restart
07.11.	0:10	12:18	0.05	3 times CM-Recovery-Action
	6:35	7:07	0.53	PC restart after running very slowly
	20:41	21:39	0.97	Windows application stuck, PC-restart
08.11.	6:04	6:20	0.27	Restart Hydromap Control
	7:55	23:36	0.08	5 times CM-Recovery-Action
09.11.	2:56	13:47	0.15	9 times CM-Recovery-Action
10.11.	1:27	16:37	0.2	12 times CM-Recovery-Action
	17:50	20:12	2.37	Cannot connect to Database, Restart Hydromap Control. Switch on/off invalid. Manual restart of CM and reconect via Hydromap Control. No

				CM messages. Reboot LAN router did not help.
11.11.	3:39	6:07	0.08	5 times CM-Recovery-Action
12.11.	15:51	17:29	0.03	2 times CM-Recovery-Action
13.11.	2:45	16:05	0.08	5 times CM-Recovery-Action
14.11.	0:16	17:11	0.1	6 times CM-Recovery-Action
	18:03	18:26	0.38	Windows application stuck. Restart Parastore
15.11.	6:13	8:43	2.5	Network communication problem, no echo, no data. Systen restarted 3x completely. Manual CM restart. Switch on/off invalid. Reconnect via Hydromap Control. No CM messages.
	11:28	12:00	0.53	Windows Application stuck, Restart Parastore
	2:41	23:07	0.08	5 times CM-Recovery-Action
16.11.	2:46	22:36	0.05	3 times CM-Recovery-Action
17.11.	1:17	22:12	0.08	5 times CM-Recovery-Action
	23:33	00:06	0.55	Windows application stuck, restart Parastore
18.11.	1:24	19:22	0.13	8 times CM-Recovery-Action
19.11.	0:06	22:31	0.15	9 times CM-Recovery-Action
20.11.	2:04	7:27	0.08	5 times CM-Recovery-Action
21.11.	1:39	6:08	0.07	4 times CM-Recovery-Action
22.11.	0:37	22:43	0.15	9 times CM-Recovery-Action
23.11.	1:29	19:46	0.12	7 times CM-Recovery-Action
24.11.	1:14	20:46	0.2	12 times CM-Recovery-Action
25.11.	0:01	20:59	0.1	6 times CM-Recovery-Action
26.11.	10:24	21:52	0.03	2 times CM-Recovery-Action
27.11.	0:55	1:51	0.93	System crash and restart
	0:36	7:53	0.08	5 times CM-Recovery-Action
28.11.	3:49			Windows / Parastore application stuck
				End of expedition data starage
28.10.	16:25	19:28	3.05	CTD-Station
07.11.	13:08	15:52	2.73	CTD-Station
27.11.	10:44	13:38	2.9	CTD-Station
sum of time without data (h)		17.93		Due to system crashes and CM recoveries, without stations
sum of time without data (h)		12.95		System crashes only
sum of station time (h)		8.68		System on Standby
Sum of operation time (h)		825.92		Including operation time without stations

Data quality was good to very good as long as the ship's motion was moderate or small. A significant decrease in data quality (signal to noise ratio) up to poor or zero is correlated with an increase of rolling motion of the ship, in particular if rolling angles of +/- 10° were exceeded (Fig. 5.8). Mostly, this was the case when total wave heights exceeded 5 m and wind force increased to 8 Bft or more and the ships heading was nearly 90° to the moving direction of the swell. As westerly to south-westerly wind-sea and swell directions

predominated during the cruise, some of the SSE-NNW (ore vice versa) profiles were effected most by deterioration in data quality. In order to partly compensate the problem we have temporally and on demand increased the periods of pulses from 2 to 4, in a few rare cases up to 16. We were not able to distinguish whether the effects were caused by increased noise level (breaking of the sea combined with acoustic interferences with the hull), increased bubbles under the transducer plate, insufficient motion compensation of the signal (transmission and reflection), or any type of combination of the above. Similar deterioration in data quality was also observed in swath bathymetric data of the independent SIMRAD System EM-120 (see Chapter 5.2 Swath Bathymetry). Thus, the causes are more likely to be ship specific rather than system specific.

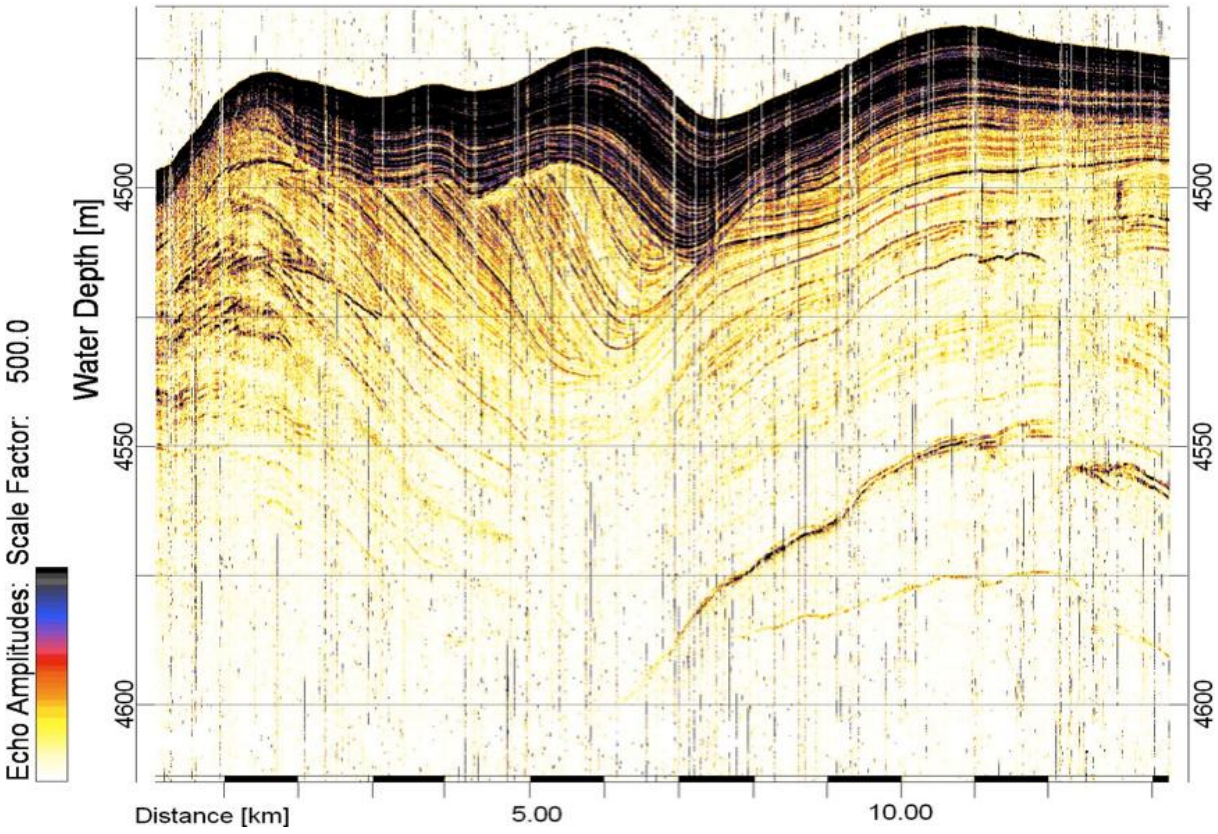

Fig. 5.12: PARASOUND profile recorded on seismic line AWI-20110402 (31.10.2011, 15:25 - 16:52 UTC) western area under investigation, Agulhas Basin. Plot produced using SeNT software.

5.3.4 Examples of recorded data along the cruise track

In the area under investigation the sediments resolved in PARASOUND profiles appear patchy as isolated, linked or stacked drift deposits. They show widespread evidence of bottom current activity and its variation with time. In most locations this is documented in variable thicknesses of sediment packages over relatively short lateral distances, which is typical for sedimentary drift or contourite deposits (Wildeboer Schut et al., 2002). We have

passed across ODP sites 1089, 1090 and 1088 (Gersonde et al., 1999) in order to provide data for linking the stratigraphy and chronology of the cores to the PARASOUND records. Sites 1089 and 1090 are in the western working area, Site 1088 is in the eastern working area (Fig. 5.3). In comparison to the seismic profiles, PARASOUND provides a higher resolution of the uppermost seismic units, namely above seismic reflectors M and P as described in previous publications about the working area (Wildeboer Schut and Uenzelmann-Neben, 2005; Wildeboer Schut et al., 2002)

In the Cape Basin at Site 1089, the PARASOUND penetration is about 100 m into well-stratified pelagic sediments (Fig. 5.9), which exhibit very little variation in sediment thickness over a lateral distance of 8 km. In the vicinity of the drill site a few debris-flow deposits are intercalated with pelagic muds, which are, in places, associated with erosion (Fig. 5.9). If not influenced by debris flows, the paleo-bathymetry is very regular leading to a symmetrical geometry of the pelagic sequence. At the drillsite the entire PARASOUND record is undisturbed. The core has a total length of 270 m and consists of interlayered nannofossil ooze and diatom mud (Gersonde et al., 1999; Wildeboer Schut and Uenzelmann-Neben, 2006).The Pleistocene-Pliocene Boundary was drilled at a depth of 230 mbsf without hiatus.

In a small sub-basin within the complex bathymetry of the western Agulhas Ridge at Site 1090, the PARASOUND penetration is about 80 m (Fig. 5.10). The sediments are well stratified and appear undisturbed. The drilled sedimentary feature is about 6 km wide and slightly asymmetrical in geometry and can be described as a small-scale moanded drift. Sediment thickness is slightly variable with respect to both space and time leading to lateral crest and moat migration (Fig. 5.10). The core has a total length of 400 m and a basal age of middle Eocene. The upper part of the cored record penetrated by PARASOUND consists of muddy diatom ooze (Miocene) overlain by calcareous ooze (Pliocene-Pleistocene). The Pleistocene-Pliocene and Pliocene-Miocene boundaries were drilled at 45 mbsf and 70 mbsf, respectively. Both boundaries are characterized by hiatuses (Gersonde et al., 1999; Wildeboer Schut and Uenzelmann-Neben, 2006), which is not obvious in the PARASOUND record (Fig. 5.10).

On the eastern Agulhas Ridge at Site 1088, the PARASOUND penetration is relatively shallow. An uppermost sediment unit of 25 m thickness reflected most of acoustic energy of the 4 kHz pulses. Thus, very strong reflectors near the top mask most of the deeper sub-bottom structures (Fig. 5.11). The uppermost unit thins out between 2150 and 2200 m water depth so that deeper penetration to 150 m becomes possible in the vicinity of the drill site. This exhibits a lenticular sedimentary drift feature of which the upper 200 m are somewhat resolved by PARASOUND (Fig. 5.11). Site 1088 is almost on top of the structure. The core has a total length of 235 m and reached a basal age of middle Miocene. The upper part of the cored record penetrated by PARASOUND consists of nannofossil foraminiferal ooze with a significant increase of foraminfera at 25 mbsf (Gersonde et al., 1999; Wildeboer Schut and Uenzelmann-Neben, 2006). The Pleistocene-Pliocene Boundary is at 25 mbsf which correlates with the strong increase in reflection coefficients as described above. The Pliocene-Miocene Boundary was drilled at 44 mbsf, of which a correlation to PARASOUND reflectors may become possible after more processing of the acoustic data.

The main difference between the western and eastern working areas is the fact that sediments with significant thicknesses covering larger areas are only present on the eastern Agulhas Ridge. One of the best examples is the sediment drift at ODP site 1088 as described above. In contrast, in the western part of the ridge, mostly no sediment coverage is indicated by PARASOUND on the peaks and flanks with ODP site 1090 as a local exception. In many locations (for example in the Agulhas Basin, Fig. 5.12) it is clearly visible that sedimentation in drifts may be interrupted by erosion. The related unconformity may form the base for younger drift deposit then often forming the uppermost acoustic unit in the area of investigation. Sediment truncation is also visible in the uppermost deposits and appear to be related to recent or very young bottom currents strong enough for eroding sediments. This observation is often related to the presents of seamounts where current velocity may be increased by focusing effects caused by the local bathymetry (Fig. 5.13).

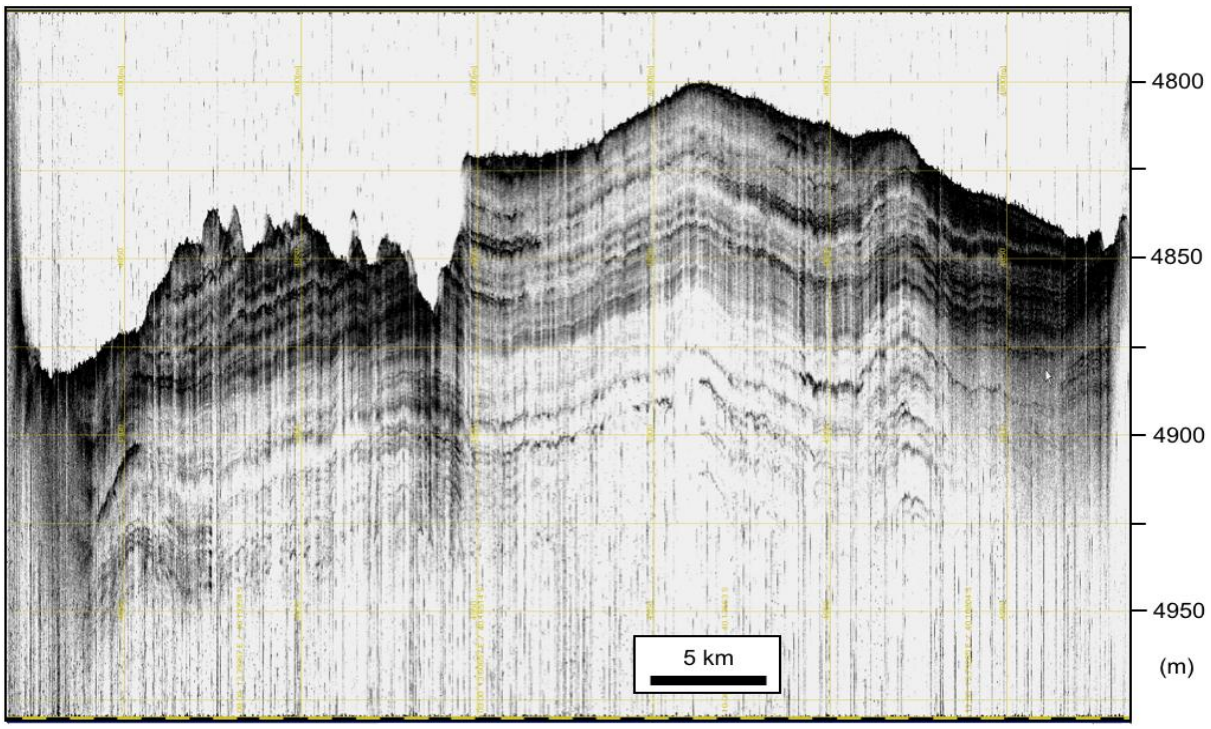

Fig. 5.13: PARASOUND profile recorded on seismic line AWI-20110412 (15.11.2011, 07:05-11:00 UTC) eastern area under investigation, Cape Basin. Plot produced using ATLAS PARASTORE-3 software (lateral scale reduction by merging two traces to one).

5.3.5 List of Abbreviations

ASCII	American Standard Code for Information Interchange
ASD	Atlas Sounding Data
C	Water sound velocity
CM	Control Module
EEZ	Exclusive Economic Zone
mbsf	Meters below Sea Floor
PHF	Primary High Frequency

P-SBP	Parametric Sub-bottom Profiling
PS3	Export format of PARASOUND data
P70	Product version of PARASOUND with 70 kW pulse transmission power
RV	Research Vessel
SBES	Single-Beam Echo-Sounder
SEG-Y	Society of Exploration Physicists-Standard Format for Seismic Data
SHF	Secondary High Frequency
SLF	Secondary Low Frequency
SM-120	Multi-Beam System (SIMRAD Echosounder)
SPM	Signal Processing Module
USB	Universal Serial Board

5.4 CTD System

(A. Müller-Michaelis)

5.4.1 Method

Water masses from different origin regions determine depth profiles in temperature and salinity. The changing hydrographic properties of the water masses in the investigation area result also in different sound velocity depth profiles. The multi-beam system uses a fixed sound velocity of 1500 m/s for profiling the sea bottom. To get better results during the MSM 19/2 cruise and for the data processing the true sound velocity profiles of different CTD (Conductivity, Temperature, Depth) reference stations are used for the calibration of these acoustic systems. The CTD consists of conductivity, temperature, and pressure sensors. The depth is evaluated by the pressure and the salinity by the conductivity. The CTD is fixed on a frame with an altimeter and niskin bottles for water samples. It is lowered by winch down to approx. 10 m above sea bottom. The profiles are measured and recorded during the down- and the up-cast. For the multi-beam system just the down casts were used and updated during the cruise. 3 CTD casts were completed on this cruise. The casts were initiated and terminated on deck. 2-4 water samples were taken per cast for calibration of the conductivity sensor.

5.4.2 Equipment

24 bottle stainless steel frame configured in the following way:

Seabird 911 plus CTD
Seabird SBE-32 position carousel
24 x 10 L HYDROBIOS-FREEFLOW “niskin” bottles

5.4.3 Preliminarily Results

List of the CTD stations:

Table 5.5: CTD station coordinates.

Cast No.	Date	Start time	Latitude	Longitude
1	10/28/2011	16:28	41° 59.980'S	9° 20.530'E
2	11/7/2011	13:08	42° 44.831'S	7° 28.548'E
3	11/27/2011	10:35	38° 24.296'S	13° 37.499'E

5.5 ADCP

(A. Müller-Michaelis)

5.5.1 Method

The vessel mounded Acoustic Doppler Current Profiler (ADCP) measures the current velocity beneath the ship using the Doppler Effect. Four beams of low-frequency acoustic signals are sent into the water column and the echo from suspended scatterers like plankton, faecal pellets etc. are evaluated to receive the velocity along the beam direction as the frequency of (sound) waves is changed by relative motion. The first pair of beams calculates east-west and vertical velocity, the second pair of beams the north-south and also the vertical velocity. The difference between two vertical velocities gives the error velocity. To get the true current velocities beneath the ship, the measured values have to be corrected for the pitch and roll movement of the ship, rotated from the ADCP coordinates to earth coordinates and the ships velocity and the tidal currents have to be subtracted.

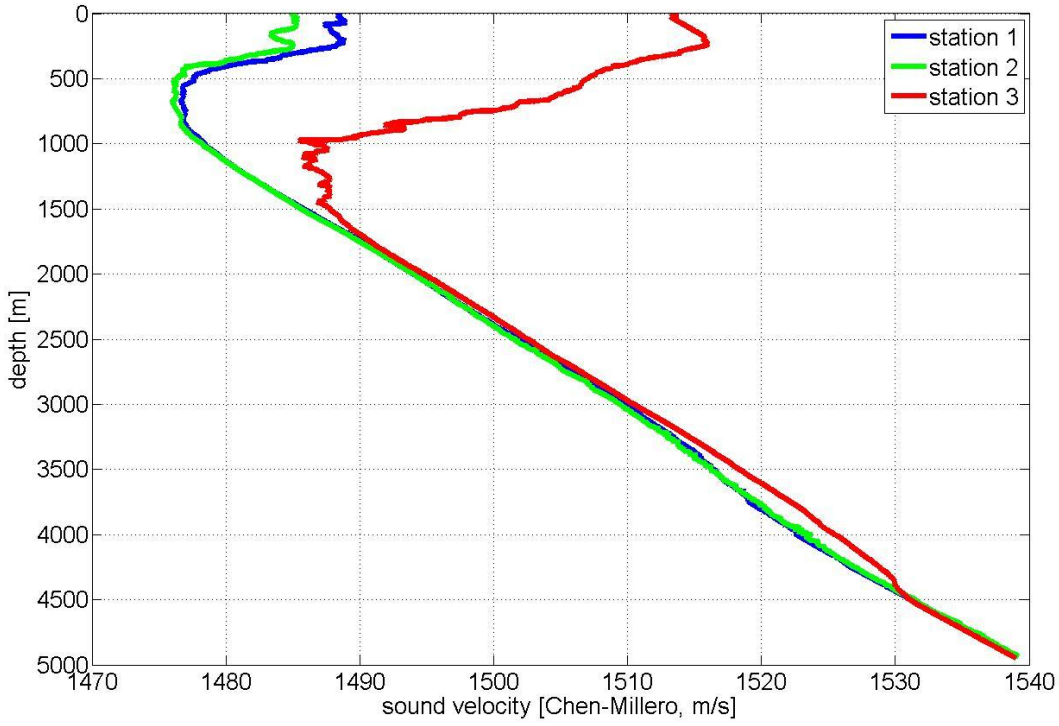

Fig. 5.14: Sound velocity profiles of the 3 CTD stations MSM 19/2.

5.5.2 Equipment

The two ship's ADCPs, which have been manufactured by RD Instruments (Poway, Ca., USA), have working frequencies of 75 kHz and 38 kHz with ping rates of 0.7 Hz and are specified for a maximal ship speed of 22 kn. Despite the fact that these instruments are

specified for a maximal bottom track depth of 950 m, the operational maximal bottom search depth was set to 500 m. A constant salinity of 35 was utilized to calculate the velocities.

5.6.3 Preliminarily results

The ADCPs had been running almost constantly during the cruise with just 2 smaller problems, which caused data gaps of a few minutes in ADCP 75 kHz data and about 30 minutes in ADCP 38 kHz data and (see tables below). The measurements were stopped and restarted every 1 to 2 days to keep the file size easily processable and to avoid data loss in cases of problems. Onboard processing of the ADCP data was not possible due to software problems.

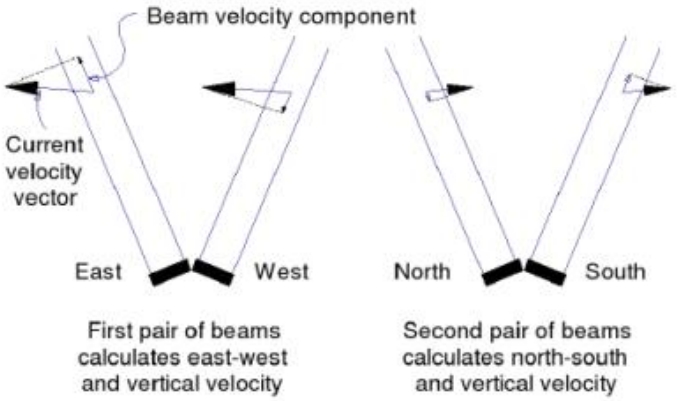

Table 5.6: Details of ADCP recording.

Profile No	Start Date	Start Time UTC	Start Latitude	Start Longitude	Stop Date	Stop Date	Stop Time UTC	Stop Latitude	Stop Longitude
1	10/24/2011	10:58	23° 24.080' S	14° 13.620' E	10/25/2011	10/25/2011	6:07	27° 10.562' S	13° 04.424' E
2	10/25/2011	6:08	27° 10.562' S	13° 04.424' E	10/26/2011	10/26/2011	6:15	31° 59.163' S	11° 55.811' E
3	10/26/2011	6:15	31° 59.163' S	11° 55.811' E	10/27/2011	10/27/2011	6:16	35° 56.411' S	10° 56.895' E
4	10/27/2011	6:16	35° 56.411' S	10° 56.895' E	10/28/2011	10/28/2011	6:50	40° 11.739' S	9° 50.141' E
5	10/28/2011	6:50	40° 11.739' S	9° 50.141'E	10/29/2011	10/29/2011	18:17	43° 52.085' S	8° 22.512' E
6	10/29/2011	18:17	43° 52.085' S	8° 22.512' E	10/30/2011	10/30/2011	7:40	42° 49.788' S	7° 46.397' E
7	10/30/2011	7:40	42° 49.788' S	7° 46.397' E	10/31/2011	10/31/2011	6:40	43° 03.010' S	8° 08.422' E
8	10/31/2011	6:41	43° 03.010' S	8° 08.422' E	11/2/2011	11/2/2011	8:53	41° 38.710' S	8° 45.353' E
9	11/2/2011	8:53	41° 38.710' S	8° 45.353' E	11/3/2011	11/3/2011	7:06	42° 48.787' S	10° 05.214' E
10	11/3/2011	7:06	42° 48.787' S	10° 05.214' E	11/4/2011	11/4/2011	8:57	42° 42.661' S	10° 35.497' E
11	11/4/2011	8:57	42° 42.661' S	10° 35.497' E	11/5/2011	11/5/2011	6:41	40° 58.444' S	9° 54.201' E
12	11/5/2011	6:41	40° 58.444' S	9° 54.201' E	11/6/2011	11/6/2011	15:21	42° 33.442' S	7° 31.573' E

13	11/6/2011	15:21	42° 33.442' S	7° 31.573' E	11/7/2011	11/7/2011	14:50	42° 44.824' S	7° 28.560' E
14	11/7/2011	14:50	42° 44.824' S	7° 28.560' E	11/9/2011	11/9/2011	9:30	41° 58.274' S	9° 50.255' E
15	11/9/2011	9:30	41° 58.274' S	9° 50.255' E	11/10/2011	11/10/2011	8:12	42° 21.975' S	10° 26.858' E
16	11/10/2011	8:12	42° 21.975' S	10° 26.858' E	11/11/2011	11/11/2011	15:16	42° 41.020' S	8° 40.900' E
17	11/11/2011	15:16	42° 41.020' S	8° 40.900' E	11/12/2011	11/12/2011	11:27	41° 44.910' S	8° 54.964' E
18	11/12/2011	11:27	41° 44.910' S	8° 54.964' E	11/13/2011	11/13/2011	7:51	41° 01.927' S	10° 57.170' E
19	11/13/2011	7:51	41° 01.927' S	10° 57.170' E	11/15/2011	11/15/2011	9:38	39° 50.222' S	15° 14.435' E
20	11/15/2011	9:38	39° 50.222' S	15° 14.435' E	11/17/2011	11/17/2011	13:34	40° 23.515' S	13° 53.074' E
21	11/17/2011	13:34	40° 23.515' S	13° 53.074' E	11/18/2011	11/18/2011	18:20	39° 27.929' S	13° 13.222' E
22	11/18/2011	18:20	39° 27.929' S	13° 13.222' E	11/19/2011	11/19/2011	8:25	40° 12.266' S	14° 22.575' E
23	11/19/2011	8:25	40° 12.266' S	14° 22.575' E	11/20/2011	11/20/2011	9:30	39° 48.097' S	14° 22.721' E
24	11/20/2011	9:30	39° 48.097' S	14° 22.721' E	11/22/2011	11/22/2011	8:05	39° 28.603' S	14° 41.839' E
25	11/22/2011	8:05	39° 28.603' S	14° 41.839' E	11/23/2011	11/23/2011	9:14	40° 52.089' S	14° 36.474' E
26	11/23/2011	9:14	40° 52.089' S	14° 36.474' E	11/24/2011	11/24/2011	8:24	40° 48.073' S	13° 14.898' E
27	11/24/2011	8:24	40° 48.073' S	13° 14.898' E	11/25/2011	11/25/2011	19:32	39° 00.534' S	14° 33.981' E
28	11/25/2011	19:32	39° 00.534' S	14° 33.981' E	11/26/2011	11/26/2011	16:54	39° 18.012' S	12° 37.621' E
29	11/26/2011	16:54	39° 18.012' S	12° 37.621' E	11/26/2011	11/26/2011	16:57	Acquisition error	
30	11/26/2011	16:57	39° 18.012' S	12° 37.621' E	11/27/2011	11/27/2011	14:35	38° 15.987' S	13° 46.164' E

6 References

Ben Avraham, Z., Hartnady, C.H.J. and Kitchin, K.A., 1997. Structure and tectonics of the Agulhas-Falkland fracture zone. Tectonophysics, 282: 83-98.

Galeotti, S., Coccioni, R. and Gersonde, R., 2002. Middle Eocene-Early Pliocene Subantarctic planktic foraminiferal biostratigraphy of Site 1090, Agulhas Ridge. Marine Micropaleontology, 45(3-4): 357-381.

Gersonde, R., Hodell, D.A., Blum, P. and al., e., 1999. Proceedings of the Ocean Drilling Program - Initial Reports. In: T.A.M. University (Editor). Ocean Drilling Program.

Hartnady, C.J.H. and le Roex, A.P., 1985. Southern Ocean hotspot tracks and the Cenozoic absolute motion of the African, Antarctic, and South American plates. Earth and Planeatry Science Letters, 75: 245-257.

Kastens, K., 1987. A compendium of causes and effects of processes at transform faults and fracture zones. Reviews of Geophysics, 25: 1554-1562.

Keller, G., 1987. Paleodepth distribution of Neogene deep-sea hiatuses. Palaeogeography, 2: 697–713.

Klages, M. and Thiede, J., 2010. The expeditions ARKTIS-XXII/1a-c of the research vessel "Polarstern" in 2007.

LaBrecque, J.L. and Hayes, D., 1979. Seafloor spreading history of the Agulhas Basin. Earth and Planetary Science Letters, 45: 411-423.

Ledbetter, M.T. and Ciesielski, P.F., 1982. Bottom-current erosion along a traverse in the south Atlantic sector of the Southern Ocean. Marine Geology, 46: 329–341.

Marino, M. and Flores, J.-A., 2002. Middle Eocene to early Oligocene calcareous nannofossil stratigraphy at Leg 177 Site 1090. Marine Micropaleontology, 45(3-4): 383-398.

Marks, K.M. and Stock, J.M., 2001. Evolution of the Malvinas Plate South of Africa. Marine Geophysical Researches, 22: 289–302.

Marks, K.M. and Tikku, A.A., 2001. Cretaceous reconstructions of East Antarctica, Africa and Madagascar. Earth and Planetary Science Letters, 186: 479-495.

Schiel, S., 2009. The expedition of the research vessel "Polarstern" to the Antarctic in 2007 (ANT-XXIV/1).

Shipboard Scientific Party, 1999a. Site 1088. In: T.A.M. University (Editor). Ocean Drilling Program.

Shipboard Scientific Party, 1999b. Site 1089. In: T.A.M. University (Editor). Ocean Drilling Program.

Shipboard Scientific Party, 1999c. Site 1090. In: T.A.M. University (Editor). Ocean Drilling Program.

Tucholke, B.E., Houtz, R.E. and Barrett, D.M., 1981. Continental crust beneath the Agulhas Plateau, Southwest Indian Ocean. Journal of Geophysical Reseach, B86: 3791-3806.

Uenzelmann-Neben, G. and Gohl, K., 2005. The Agulhas Ridge, South Atlantic: the peculiar structure of a fracture zone. Marine Geophysical Research, 25: 305-319.

Venz, K.A. and Hodell, D.A., 2002. New evidence for changes in Plio-Pleistocene deep water circulation from Southern Ocean ODP Leg 177 Site 1090. Palaeogeography, Palaeoclimatology, Palaeoecology, 182(3-4): 197-220.

Wildeboer Schut, E. and Uenzelmann-Neben, G., 2005. Cenozoic bottom current sedimentation in the Cape Basin, South Atlantic. Geophysical Journal International, 161: 325-333.

Wildeboer Schut, E. and Uenzelmann-Neben, G., 2006. Tying seismic data to geologic information from core data: An example from ODP Leg 177. Geo-Marine Letters, 26: 235-248.

Wildeboer Schut, E., Uenzelmann-Neben, G. and Gersonde, R., 2002. Seismic evidence for bottom current activity at the Agulhas Ridge. Global and Planetary Change, 34: 185-198.

Zielinski, U. and Gersonde, R., 2002. Plio-Pleistocene diatom biostratigraphy from ODP Leg 177, Atlantic sector of the Southern Ocean. Marine Micropaleontology, 45(3-4): 225-268.

7 Acknowledgements

We like to thank Captain Friedrich von Staa, his officers and crew of RV *Maria S. Merian* for their support of our measurement programme and for creating a very friendly atmosphere on board.

The ship time of FS *Maria S. Merian* was provided by the Deutsche Forschungsgemeinschaft within the core program METEOR/MERIAN. We also benefited from financial contributions by the research institutes involved. We gratefully acknowledge all this support.

Appendix 1 Teilnehmende Institute/ Participating Institutions

AWI	Alfred-Wegener-Institut für Polar- und Meeresforschung in der Helmholtz-Gemeinschaft Am Alten Hafen 26, D-27568 Bremerhaven, Germany (www.awi.de)
IFM-GEOMAR	Leibniz-Institut für Meereswissenschaften Wischofstr. 1-3 24148 Kiel, Germany www.ifm-geomar.de
Optimare	OPTIMARE Sensorsysteme AG Am Loners 15a, D-27572 Bremerhaven, Germany (www.optimare.de)
UCT	University of Cape Town,Department of Geological Sciences Rondebosch 7700, South Africa

Appendix 2 Fahrtteilnehmer / Cruise Participants

UENZELMANN-NEBEN, Gabriele	Chief Scientist	AWI
CAWTHRA, Hayley	student, Seismics	UCT
DUFEK, Tanja	Simrad	AWI
EGGERS, Thorsten	Seismics	Optimare
FREUND, Madeleine	student, PARASOUND	AWI
GRÜTZNER, Jens	Seismics	AWI
HORN, Michael	student, Seismics	AWI
MÜLLER-MICHAELIS, Antje	student, Seismics	AWI
NIESSEN, Frank	PARASOUND	AWI
PENSHORN, Dietmar	Seismics	AWI
SANZ, Christopher	student, PARASOUND	AWI
SEIDEL, Elisabeth	student, Seismics	AWI
SUCKRO, Sonja	student, Seismics	AWI
WERNER, Reinhard	Simrad	IfM-GEOMAR
MÜLLER, Reinhard	doctor	Briese

Appendix 3 Besatzung / Ship's Crew

VON STAA, Friedhelm	Master
MAASS, Björn	Chief Officer
GÜNTHER, Jan Philipp	1st Officer
STEGMAIER, Eberhard	2nd Officer
OGRODNIK, Thomas	Chief Engineer
ROGERS, Benjamin	2nd Engineer
PLATHE, Hans-Dieter	3rd Engineer
SCHMIDT, Hendrik	Electrician
FRIESENBORG, Helmut	Fitter
MEINECKE, Stefan	Electronics
TOMIAK, Martin	SysOps
BOSSELMANN, Norbert	Bosun
ROOB, Christian	AB
VREDENBORG, Enno	AB
SCHRAGE, Frank	AB
PETERS, Karsten	AB
ZERSEN, Hendrik	AB
WOLF, Andreas	AB
PESCHEL, Jens	AB
SAUER, Jürgen	Oiler
ARNDT, Waldemar	Cook
KROEGER, Sven	2nd Cook
JORDAN, Dieter	Steward

Appendix 4 Stationsliste / Station List

Station No.	Date	Time [UTC]	Position Lat	Position Lon	Depth [m]	Gear	Action	Comment
MSM19/1068-1	10/28/2011	16:29	41° 59,98' S	9° 20,54' E	4785	CTD/rosette water sampler	surface	
MSM19/1068-1	10/28/2011	17:52	41° 59,99' S	9° 20,54' E	4783.6	CTD/rosette water sampler	at depth	SL max 4765m
MSM19/1068-1	10/28/2011	19:23	41° 59,99' S	9° 20,54' E	4785.6	CTD/rosette water sampler	on deck	
MSM19/1069-1	10/29/2011	7:25	44° 8,73' S	8° 52,06' E	4570.6	Seismic reflection profile	information	Beginn aussetzen Streamer
MSM19/1069-1	10/29/2011	8:40	44° 13,50' S	8° 49,63' E	4562	Seismic reflection profile	Streamer into water	SL max 3192
MSM19/1069-1	10/29/2011	8:58	44° 14,62' S	8° 49,04' E	4561.3	Seismic reflection profile	airguns in the water	
MSM19/1069-1	10/29/2011	11:45	44° 21,71' S	8° 40,45' E	4461.6	Seismic reflection profile	profile start	Kurs 337°
MSM19/1069-1	10/29/2011	15:13	44° 5,83' S	8° 31,04' E	4417.2	Seismic reflection profile	information	Schießen unterbrochen, austausch der Blasen an den Kanonen
MSM19/1069-1	10/29/2011	15:52	44° 3,35' S	8° 29,59' E	14.2	Seismic reflection profile	information	Blasen ausgetauscht
MSM19/1069-1	10/29/2011	16:00	44° 2,81' S	8° 29,27' E	4500.7	Seismic reflection profile	information	Fortsetzen Schießen
MSM19/1069-1	10/30/2011	11:05	42° 33,91' S	7° 37,21' E	4705.5	Seismic reflection profile	information	Schießpause wegen Triggertausch
MSM19/1069-1	10/30/2011	11:08	42° 33,68' S	7° 37,09' E	5389.7	Seismic reflection profile	information	Fortsetzung schießen
MSM19/1069-1	10/30/2011	15:06	42° 15,20' S	7° 26,41' E	4762.9	Seismic reflection profile	end of profile	
MSM19/1069-1	10/30/2011	15:29	42° 13,42' S	7° 25,35' E	4750.7	Seismic reflection profile	alter course	Neuer Kurs 147°
MSM19/1069-1	10/30/2011	18:42	42° 15,13' S	7° 26,37' E	4890	Seismic reflection profile	profile start	
MSM19/1069-1	10/31/2011	10:16	43° 17,61' S	8° 21,34' E	3107.9	Seismic reflection profile	information	Kursänderung nach Bb um Datenübertragung zu ermöglichen
MSM19/1069-1	10/31/2011	10:30	43° 18,51' S	8° 22,32' E	3900.6	Seismic reflection profile	information	Rückkehr auf Profil
MSM19/1069-1	10/31/2011	10:54	43° 20,20' S	8° 23,75' E	4298.4	Seismic reflection profile	information	erneute Abweichung gen Bb zwecks Datenübertragung
MSM19/1069-1	10/31/2011	11:08	43° 21,08' S	8° 24,82' E	3927.8	Seismic reflection profile	information	Drehen wieder auf Kurs
MSM19/1069-1	10/31/2011	23:01	44° 10,84' S	9° 8,90' E	4661.1	Seismic reflection profile	end of profile	
MSM19/1069-1	10/31/2011	23:02	44° 10,91' S	9° 8,97' E	4660.3	Seismic reflection profile	alter course	Neuer Kurs 352°
MSM19/1069-1	11/1/2011	2:10	44° 10,84' S	9° 8,83' E	4660	Seismic reflection profile	profile start	

Station No.	Date	Time [UTC]	Position Lat	Position Lon	Depth [m]	Gear	Action	Comment
MSM19/1069-1	11/1/2011	17:38	42° 54,61' S	8° 54,00' E	3701.4	Seismic reflection profile	alter course	Neuer Kurs 355°
MSM19/1069-1	11/2/2011	9:28	41° 35,92' S	8° 45,06' E	4925.2	Seismic reflection profile	end of profile	
MSM19/1069-1	11/2/2011	9:52	41° 33,95' S	8° 44,84' E	5047.3	Seismic reflection profile	alter course	neuer Kurs 141°
MSM19/1069-1	11/2/2011	12:09	41° 35,91' S	8° 44,98' E	4646.7	Seismic reflection profile	profile start	
MSM19/1069-1	11/3/2011	10:02	43° 0,04' S	10° 17,69' E	4219.1	Seismic reflection profile	information	Kursänderung nach Bb um Datenübertragung zu ermö
MSM19/1069-1	11/3/2011	10:48	43° 2,95' S	10° 20,97' E	3959.1	Seismic reflection profile	information	wieder auf Profilkurs
MSM19/1069-1	11/3/2011	14:03	43° 15,45' S	10° 34,88' E	4352.2	Seismic reflection profile	information	vorübergehende Kusänderung um Daten zu übertragen Kurs 132°
MSM19/1069-1	11/3/2011	14:15	43° 16,19' S	10° 35,75' E	4328.7	Seismic reflection profile	information	Zurück auf Kurs 141°
MSM19/1069-1	11/3/2011	18:00	43° 30,63' S	10° 51,87' E	4510.4	Seismic reflection profile	information	vorübergehende Kursänderung auf 131° zwecks Datenaustausch
MSM19/1069-1	11/3/2011	18:35	43° 32,80' S	10° 54,36' E	4461.2	Seismic reflection profile	information	zurück auf Kurs 141°
MSM19/1069-1	11/3/2011	19:06	43° 34,83' S	10° 56,56' E	4491.9	Seismic reflection profile	end of profile	
MSM19/1069-1	11/3/2011	19:30	43° 36,37' S	10° 58,28' E	4535.5	Seismic reflection profile	alter course	neuer Kurs 343°
MSM19/1069-1	11/3/2011	22:16	43° 34,88' S	10° 56,60' E	4906.7	Seismic reflection profile	profile start	
MSM19/1069-1	11/5/2011	7:06	40° 56,47' S	9° 53,44' E	4637.8	Seismic reflection profile	end of profile	
MSM19/1069-1	11/5/2011	7:30	40° 54,53' S	9° 52,71' E	14.2	Seismic reflection profile	alter course	neuer Kurs 227°
MSM19/1069-1	11/5/2011	9:37	40° 53,30' S	9° 56,50' E	4606.5	Seismic reflection profile	profile start	
MSM19/1069-1	11/5/2011	10:54	40° 57,69' S	9° 50,23' E	4649.1	Seismic reflection profile	information	Kursänderung für e-mail Übertragung
MSM19/1069-1	11/5/2011	11:09	40° 58,53' S	9° 48,98' E	4670.1	Seismic reflection profile	information	wieder auf Profil
MSM19/1069-1	11/5/2011	13:35	41° 6,87' S	9° 37,08' E	4667.2	Seismic reflection profile	information	Ein Kanonenauftriebskörper losgerissen
MSM19/1069-1	11/5/2011	13:50	41° 7,66' S	9° 35,96' E	4715.3	Seismic reflection profile	airgun on deck	
MSM19/1069-1	11/5/2011	14:36	41° 9,71' S	9° 32,99' E	4688.1	Seismic reflection profile	airguns in the water	Fortsetzen Schießen
MSM19/1069-1	11/6/2011	17:43	42° 41,51' S	7° 19,75' E	5149.5	Seismic reflection profile	end of profile	
MSM19/1069-1	11/6/2011	18:07	42° 42,89' S	7° 17,74' E	4948.9	Seismic reflection profile	information	aufgehört zu schießen

Station No.	Date	Time [UTC]	Position Lat	Position Lon	Depth [m]	Gear	Action	Comment
MSM19/1069-1	11/6/2011	19:02	42° 42,64' S	7° 12,73' E	4661.8	Seismic reflection profile	airgun on deck	
MSM19/1069-1	11/6/2011	19:53	42° 41,12' S	7° 8,91' E	4734.3	Seismic reflection profile	streamer on deck	
MSM19/1069-2	11/7/2011	13:13	42° 44,83' S	7° 28,54' E	4945.1	CTD/rosette water sampler	surface	
MSM19/1069-2	11/7/2011	14:17	42° 44,82' S	7° 28,55' E	4956.7	CTD/rosette water sampler	at depth	SL max. 4946m
MSM19/1069-2	11/7/2011	15:33	42° 44,82' S	7° 28,56' E	4948.3	CTD/rosette water sampler	on deck	
MSM19/1070-1	11/8/2011	6:07	42° 43,00' S	7° 31,30' E	4588.4	Seismic reflection profile	information	Beginn Aussetzen Streamer
MSM19/1070-1	11/8/2011	7:11	42° 43,78' S	7° 25,70' E	4886.4	Seismic reflection profile	Streamer into water	SL max. 3191m
MSM19/1070-1	11/8/2011	7:38	42° 44,19' S	7° 23,32' E	4789.5	Seismic reflection profile	airguns in the water	Bb-Seite
MSM19/1070-1	11/8/2011	7:47	42° 44,45' S	7° 22,61' E	4789.4	Seismic reflection profile	information	Beginn Schießen
MSM19/1070-1	11/8/2011	9:35	42° 41,47' S	7° 19,81' E	4842.2	Seismic reflection profile	profile start	Kurs 069°
MSM19/1070-1	11/9/2011	19:39	41° 40,07' S	10° 53,14' E	4381.5	Seismic reflection profile	end of profile	
MSM19/1070-1	11/9/2011	20:03	41° 39,36' S	10° 55,62' E	4389.1	Seismic reflection profile	alter course	neuer Kurs 205°
MSM19/1070-1	11/9/2011	22:52	41° 40,03' S	10° 53,21' E	4384.1	Seismic reflection profile	profile start	
MSM19/1070-1	11/10/2011	22:52	43° 27,79' S	9° 44,89' E	4305.5	Seismic reflection profile	end of profile	
MSM19/1070-1	11/10/2011	23:17	43° 29,68' S	9° 43,72' E	4340.1	Seismic reflection profile	alter course	neuer Kurs 312°
MSM19/1070-1	11/11/2011	1:50	43° 27,92' S	9° 44,88' E	4307.9	Seismic reflection profile	profile start	
MSM19/1070-1	11/11/2011	11:52	42° 54,79' S	8° 54,27' E	3711.4	Seismic reflection profile	alter course	neuer Kurs 325°
MSM19/1070-1	11/11/2011	11:54	42° 54,67' S	8° 54,11' E	3705	Seismic reflection profile	end of profile	
MSM19/1070-1	11/11/2011	11:55	42° 54,61' S	8° 54,05' E	3701.3	Seismic reflection profile	profile start	
MSM19/1070-1	11/12/2011	0:49	42° 2,61' S	8° 4,10' E	5252.4	Seismic reflection profile	end of profile	
MSM19/1070-1	11/12/2011	1:12	42° 1,10' S	8° 2,56' E	4855.1	Seismic reflection profile	alter course	neuer Kurs 065°
MSM19/1070-1	11/12/2011	3:01	42° 2,67' S	8° 4,09' E	4764.7	Seismic reflection profile	profile start	
MSM19/1070-1	11/14/2011	1:50	40° 23,78' S	12° 44,68' E	4806.5	Seismic reflection profile	information	Kurshalten durch achterlichen Wind und Strom nur erschwert möglich

Station No.	Date	Time [UTC]	Position Lat	Position Lon	Depth [m]	Gear	Action	Comment
MSM19/1070-1	11/14/2011	5:27	40° 15,95' S	13° 6,31' E	4643.3	Seismic reflection profile	alter course	Neuer Kurs 072°
MSM19/1070-1	11/15/2011	3:42	39° 39,79' S	15° 29,48' E	4871.1	Seismic reflection profile	end of profile	
MSM19/1070-1	11/15/2011	5:04	39° 37,04' S	15° 34,19' E	4311.8	Seismic reflection profile	information	EInholen der ersten Meter des Streamers um Batterien in den Birds zu wechseln
MSM19/1070-1	11/15/2011	5:21	39° 36,55' S	15° 32,94' E	4510.3	Seismic reflection profile	airgun on deck	zu Wartungszwecken
MSM19/1070-1	11/15/2011	5:44	39° 36,75' S	15° 31,15' E	4776.2	Seismic reflection profile	information	Streamer bis zum 6. Bird an Deck
MSM19/1070-1	11/15/2011	6:27	39° 38,93' S	15° 29,01' E	4593.5	Seismic reflection profile	airguns in the water	
MSM19/1070-1	11/15/2011	6:32	39° 39,18' S	15° 28,71' E	4573.9	Seismic reflection profile	Streamer into water	SL max 3192m
MSM19/1070-1	11/15/2011	6:54	39° 40,39' S	15° 27,07' E	4689.1	Seismic reflection profile	profile start	Kurs 225°
MSM19/1070-1	11/16/2011	7:33	41° 7,77' S	13° 33,64' E	2075.3	Seismic reflection profile	alter course	neuer Kurs 219°
MSM19/1070-1	11/16/2011	7:46	41° 8,60' S	13° 32,77' E	2081	Seismic reflection profile	end of profile	
MSM19/1070-1	11/16/2011	8:12	41° 10,26' S	13° 30,96' E	2086.7	Seismic reflection profile	alter course	neuer Kurs 098°
MSM19/1070-1	11/16/2011	10:30	41° 7,66' S	13° 32,21' E	2070.3	Seismic reflection profile	profile start	
MSM19/1070-1	11/16/2011	21:44	41° 14,38' S	14° 42,99' E	4423.4	Seismic reflection profile	end of profile	
MSM19/1070-1	11/16/2011	22:08	41° 14,64' S	14° 45,62' E	4399.2	Seismic reflection profile	alter course	neuer Kurs 323°
MSM19/1070-1	11/17/2011	0:51	41° 14,43' S	14° 43,08' E	4427.1	Seismic reflection profile	profile start	
MSM19/1070-1	11/18/2011	8:03	39° 3,92' S	12° 35,97' E	4979.2	Seismic reflection profile	end of profile	
MSM19/1070-1	11/18/2011	8:26	39° 2,21' S	12° 34,38' E	4845.9	Seismic reflection profile	alter course	neuer Kurs 130°
MSM19/1070-1	11/18/2011	11:29	39° 3,88' S	12° 35,84' E	4976.2	Seismic reflection profile	profile start	
MSM19/1070-1	11/18/2011	22:46	39° 42,48' S	13° 35,90' E	4623.3	Seismic reflection profile	information	Unterbrechung Schießen, wegen Blasenverlust
MSM19/1070-1	11/18/2011	23:14	39° 43,73' S	13° 37,85' E	4672.7	Seismic reflection profile	information	Fortsetzung Profil
MSM19/1070-1	11/19/2011	12:00	40° 24,79' S	14° 42,30' E	1726.7	Seismic reflection profile	information	
MSM19/1070-1	11/19/2011	17:22	40° 43,67' S	15° 12,06' E	4446.7	Seismic reflection profile	end of profile	
MSM19/1070-1	11/19/2011	17:22	40° 43,67' S	15° 12,06' E	4446.7	Seismic reflection profile	information	Unterbrechen Schießen, Wartung der Kanonen

Station No.	Date	Time [UTC]	Position Lat	Position Lon	Depth [m]	Gear	Action	Comment
MSM19/1070-1	11/19/2011	17:23	40° 43,73' S	15° 12,15' E	4448.3	Seismic reflection profile	alter course	Neuer Kurs 326°
MSM19/1070-1	11/19/2011	17:37	40° 44,17' S	15° 13,50' E	4477.5	Seismic reflection profile	airgun on deck	
MSM19/1070-1	11/19/2011	20:27	40° 42,97' S	15° 10,53' E	4483	Seismic reflection profile	airguns in the water	
MSM19/1070-1	11/19/2011	20:32	40° 42,69' S	15° 10,30' E	4511.7	Seismic reflection profile	information	Beginn Schießen
MSM19/1070-1	11/19/2011	20:37	40° 42,35' S	15° 10,02' E	4402.3	Seismic reflection profile	profile start	
MSM19/1070-1	11/20/2011	11:13	39° 40,36' S	14° 16,06' E	4707.2	Seismic reflection profile	information	Airguns über Streamer
MSM19/1070-1	11/20/2011	11:21	39° 39,75' S	14° 15,55' E	5066.3	Seismic reflection profile	information	Airguns aus; reduzieren auf 4 kn
MSM19/1070-1	11/20/2011	11:32	39° 39,06' S	14° 15,08' E	4733.7	Seismic reflection profile	information	Streamer frei, Fahrterhöhung auf 5,5kn
MSM19/1070-1	11/20/2011	12:00	39° 37,00' S	14° 13,16' E	4793.5	Seismic reflection profile	information	Fortsetzung Schießen
MSM19/1070-1	11/21/2011	2:21	38° 18,02' S	13° 5,55' E	5091.5	Seismic reflection profile	information	Probleme mit den GPS Positionen, fahren nach FDW
MSM19/1070-1	11/21/2011	2:43	38° 16,28' S	13° 4,07' E	5085.1	Seismic reflection profile	end of profile	
MSM19/1070-1	11/21/2011	2:57	38° 15,17' S	13° 3,28' E	6087.5	Seismic reflection profile	information	GPS Geräte zeigen wieder gute Positionen
MSM19/1070-1	11/21/2011	2:58	38° 15,10' S	13° 3,23' E	5076.7	Seismic reflection profile	alter course	Neuer Kurs 133°
MSM19/1070-1	11/21/2011	6:29	38° 17,85' S	13° 5,39' E	5091.9	Seismic reflection profile	profile start	
MSM19/1070-1	11/21/2011	12:00	38° 34,25' S	13° 27,61' E	4415.7	Seismic reflection profile	information	ein Bird verloren gemeldet, hieven Streamer um nachzusehen
MSM19/1070-1	11/21/2011	12:17	38° 34,85' S	13° 28,42' E	4402.4	Seismic reflection profile	information	Beginn hieven
MSM19/1070-1	11/21/2011	12:48	38° 35,40' S	13° 29,15' E	4367.8	Seismic reflection profile	information	Defekter Bird an Deck
MSM19/1070-1	11/21/2011	13:28	38° 36,11' S	13° 30,12' E	4295.7	Seismic reflection profile	information	Streamer wird wieder ausgesteckt
MSM19/1070-1	11/21/2011	13:49	38° 36,48' S	13° 30,66' E	4249	Seismic reflection profile	information	Fortsetzung Schießen und Profil
MSM19/1070-1	11/22/2011	17:15	40° 4,84' S	15° 31,85' E	4806.5	Seismic reflection profile	end of profile	
MSM19/1070-1	11/22/2011	17:17	40° 4,98' S	15° 32,05' E	4800.6	Seismic reflection profile	alter course	Neuer Kurs 220°
MSM19/1070-1	11/22/2011	19:46	40° 3,45' S	15° 30,00' E	4831.9	Seismic reflection profile	profile start	
MSM19/1070-1	11/23/2011	15:17	41° 14,99' S	14° 11,07' E	4104.1	Seismic reflection profile	information	Druckabfall durch Defekt einer Kanone. Profil wird mir 3 Kanonen fortgesetzt

Station No.	Date	Time [UTC]	Position Lat	Position Lon	Depth [m]	Gear	Action	Comment
MSM19/1070-1	11/23/2011	19:16	41° 30,08' S	13° 54,23' E	4301.9	Seismic reflection profile	end of profile	
MSM19/1070-1	11/23/2011	19:40	41° 31,60' S	13° 52,51' E	4573.8	Seismic reflection profile	alter course	neuer Kurs 325°
MSM19/1070-1	11/23/2011	22:03	41° 30,18' S	13° 54,24' E	4314.5	Seismic reflection profile	profile start	
MSM19/1070-1	11/24/2011	3:32	41° 7,80' S	13° 33,59' E	2075.8	Seismic reflection profile	alter course	WP 1088 Neuer Kurs 324°
MSM19/1070-1	11/24/2011	16:23	40° 16,20' S	12° 44,88' E	4868.7	Seismic reflection profile	end of profile	
MSM19/1070-1	11/24/2011	16:25	40° 16,07' S	12° 44,76' E	4868.8	Seismic reflection profile	alter course	Neuer Kurs 045°
MSM19/1070-1	11/24/2011	19:05	40° 17,91' S	12° 46,35' E	4843.8	Seismic reflection profile	profile start	
MSM19/1070-1	11/25/2011	17:25	38° 59,44' S	14° 28,58' E	4762.8	Seismic reflection profile	end of profile	
MSM19/1070-1	11/25/2011	17:25	38° 59,44' S	14° 28,58' E	4762.8	Seismic reflection profile	alter course	Neuer Kurs 259°
MSM19/1070-1	11/25/2011	20:37	39° 0,93' S	14° 26,69' E	4773.9	Seismic reflection profile	profile start	
MSM19/1070-1	11/26/2011	18:34	39° 19,43' S	12° 28,60' E	5038.1	Seismic reflection profile	end of profile	
MSM19/1070-1	11/26/2011	19:02	39° 19,85' S	12° 25,96' E	5011.9	Seismic reflection profile	alter course	neuer Kurs 044°
MSM19/1070-1	11/26/2011	21:47	39° 19,46' S	12° 28,49' E	5032.5	Seismic reflection profile	profile start	
MSM19/1070-1	11/27/2011	8:31	38° 30,48' S	13° 29,82' E	5029.9	Seismic reflection profile	end of profile	
MSM19/1070-1	11/27/2011	8:54	38° 28,88' S	13° 31,83' E	4975.6	Seismic reflection profile	information	Ende Schießen
MSM19/1070-1	11/27/2011	9:03	38° 28,44' S	13° 32,35' E	4967.2	Seismic reflection profile	airgun on deck	
MSM19/1070-1	11/27/2011	10:23	38° 24,54' S	13° 37,23' E	4945	Seismic reflection profile	streamer on deck	
MSM19/1071-1	11/27/2011	10:36	38° 24,29' S	13° 37,50' E	4975.1	CTD/rosette water sampler	surface	
MSM19/1071-1	11/27/2011	12:08	38° 24,30' S	13° 37,51' E	4965.2	CTD/rosette water sampler	at depth	SL max 4954m
MSM19/1071-1	11/27/2011	13:35	38° 24,28' S	13° 37,50' E	4955.1	CTD/rosette water sampler	on deck	

Appendix 5 Seismische Parameter / Seismic recording parameters

begin				end				length [nm]	airgun conFiguration	total volume [l]	shot interval [s]	No of shots	field tapes
date	UTC	lat	lon	date	UTC	lat	lon						
29.10.11	10:03	-44.267	8.8	30.10.11	15:29	-42.21	7.42	143	4 GI-guns	9.6	10	10599	P00009
30.10.11	18:42	-42.25	7.44	31.10.11	23:00	-44.2	9.17	141	4 GI-guns	9.6	10	10335	P00009/P00006
1.11.11	2:10	-44.18	9.15	2.11.11	9:51	-41.567	8.747	154	4 GI-guns	9.6	10	11405	P00006
2.11.11	12:08	-41.598	8.748	3.11.11	19:29	-43.606	10.97	154	4/3 GI-guns	9.6/7.2	10	11387	P00006/P00011
3.11.11	22:15	-43.583	10.944	5.11.11	7:30	-40.905	9.878	162	3 GI-guns	7.2	10	11976	P00011
5.11.11	9:37	-40.888	9.942	6.11.11	18:35	-42.714	7.296	154	3 GI-guns	7.2	10	11363	P00011
7.11.11	7:46	-42.74	7.378	9.11.11	19:39	-41.666	10.89	174	3 GI-guns	7.2	10	12880	P00007
9.11.11	22:52	-41.667	10.887	10.11.11	23:17	-43.96	9.727	119	3 GI-guns	7.2	10	8788	P00007
11.11.11	1:50	-43.465	9.748	11.11.11	11:54	-42.909	8.9	50	3 GI-guns	7.2	10	3624	P00007/P00014
11.11.11	11:54	-42.909	8.9	11.11.11	1:01	-42.029	8.054	63	3 GI-guns	7.2	10	4637	P00014
12.11.11	3:01	-42.044	8.068	14.11.11	5:27	-40.265	13.107	244	3 GI-guns	7.2	10	18076	P00014/P00016
14.11.11	5:27	-40.265	13.105	15.11.11	3:29	-39.668	15.474	104	3 GI-guns	7.2	10	7677	P00016/P00008
15.11.11	6:54	-39.673	15.451	16.11.11	7:46	-41.145	13.545	121	3 GI-guns	7.2	10	8947	P00008

begin			end				length [nm]	airgun conFiguration	total volume [l]	shot interval [s]	No of shots	field tapes	Line
UTC	lat	lon	date	UTC	lat	lon							
10:30	-41.127	13.537	16.11.11	22:07	-41.244	14.761	56	3 GI-guns	7.2	10	4115	P00008	AWI-20110401
00:50	-41.241	14.719	18.11.11	8:02	-39.064	12.598	148	3 GI-guns	7.2	10	10988	P00008/P00013	AWI-20110402
11:30	-39.066	12.599	19.11.11	17:02	-40.711	15.175	142	3 GI-guns	7.2	10	10478	P00013	AWI-20110403
20:37	-40.709	15.17	21.11.11	2:43	-38.267	13.065	143	4 GI-guns	9.6	10	10627	P00013/P00010	AWI-20110404
6:27	-38.299	13.085	22.11.11	17:15	-40.083	15.533	162	4 GI-guns	9.6	10	11964	P00010/P00017	AWI-20110405
19:46	-40.057	15.5	23.11.11	19:46	-41.528	13.873	116	4/3 GI-guns	9.6/7.2	10	8584	P00017	AWI-20110406
23:03	-41.503	13.904	24.11.11	15:59	-40.295	12.772	88	3 GI-guns	7.2	10	6481	P00017	AWI-20110407
18:58	-40.305	12.763	25.11.11	17:24	-38.989	14.478	109	3 GI-guns	7.2	10	8077	P00017/P00019	AWI-20110408
20:37	-39.015	14.445	26.11.11	18:59	-39.33	12.435	109	3 GI-guns	7.2	10	8056	P00019	AWI-20110409
21:47	-39.326	12.472	27.11.11	8:52	-38.481	13.53	54	3 GI-guns	7.2	10	3995	P00019/P00018	AWI-20110410
													AWI-20110411
													AWI-20110412
													AWI-20110413

	date	16.11.11	17.11.11	18.11.11	19.11.11	21.11.11	22.11.11	23.11.11	24.11.11	25.11.11	26.11.11
Line		AWI-20110414	AWI-20110415	AWI-20110416	AWI-20110417	AWI-20110418	AWI-20110419	AWI-20110420	AWI-20110421	AWI-2011022	AWI-20110423

Die "Berichte zur Polar- und Meeresforschung" (ISSN 1866-3192) werden beginnend mit dem Heft Nr. 569 (2008) als Open-Access-Publikation herausgegeben. Ein Verzeichnis aller Hefte einschließlich der Druckausgaben (Heft 377-568) sowie der früheren **"Berichte zur Polarforschung** (Heft 1-376, von 1982 bis 2000) befindet sich im Internet in der Ablage des electronic Information Center des AWI (**ePIC Reports**) unter der URL http://epic-reports.awi.de. Durch Auswahl "Reports on Polar- and Marine Research" (via "browse"/"type") wird eine Liste der Publikationen sortiert nach Heftnummer innerhalb der absteigenden chronologischen Reihenfolge der Jahrgänge erzeugt.

To generate a list of all Reports past issues, use the following URL: http://epic-reports.awi.de and select "browse"/"type" to browse "Reports on Polar and Marine Research". A chronological list in declining order, issues chronological, will be produced, and pdf-icons shown for open access download.

Verzeichnis der zuletzt erschienenen Hefte:

Heft-Nr. 629/2011 — "Russian-German Cooperation SYSTEM LAPTEV SEA: The expedition Eastern Laptev Sea - Buor Khaya Peninsula 2010" edited by Sebastian Wetterich, Pier Paul Overduin and Mikhail Grigoriev

Heft-Nr. 630/2011 — "Comparative aerosol studies based on multi-wavelength Raman LIDAR at Ny-Ålesund, Spitsbergen", by Anne Hoffmann

Heft-Nr. 631/2011 — "The Expedition of the Research Vessel 'Polarstern' to the Antarctic in 2010 (ANT-XXVI/4), edited by Arne Körtzinger

Heft-Nr. 632/2011 — "The Expedition of the Research Vessel 'Polarstern' to the polar South Pacific in 2009/2010 (ANT-XXVI/2 - BIPOMAC), edited by Rainer Gersonde

Heft-Nr. 633/2011 — "Investigation of Katabatic winds and Polynyas during Summer – IKAPOS Field Phase Report", by Günther Heinemann, Thomas Ernsdorf and Clemens Drüe"

Heft-Nr. 634/2011 — "The Expedition of the Research Vessel 'Polarstern' to the Antarctic in 2010/11 (ANT-XXVII/2)", edited by Eberhard Fahrbach

Heft-Nr. 635/2011 — "Direkte numerische Simulation von Salzfingern", by Thomas Zweigle

Heft-Nr. 636/2011 — "The joint Russian-German Expedition BERINGIA/KOLYMA 2008 during the International Polar Year (IPY) 2007/2008", edited by Sebastian Wetterich, Lutz Schirrmeister and Aleksander L. Kholodov

Heft-Nr. 637/2011 — "The European Research Icebreaker AURORA BOREALIS Conceptual Design Study — Summary Report", edited by Lester Lembke-Jene, Nicole Biebow and Jörn Thiede

Heft-Nr. 638/2011 — "Long-term evolution of (millennial-scale) climate variability in the North Atlantic over the last four million years - Results from Integrated Ocean Drilling Project Site U1313", by Bernhard David Adriaan Naafs

Heft-Nr. 639/2011 — "The Expedition of the Research Vessel 'Polarstern' to the Antarctic in 2011 (ANT-XXVII/4)", edited by Saad El Nagger

Heft-Nr. 640/2012 — "ARCTIC MARINE BIOLOGY - A workshop celebrating two decades of cooperation between Murmansk Marine Biological Institute and Alfred Wegener Institute for Polar and Marine Research", edited by Gotthilf Hempel, Karin Lochte, Gennady Matishov

Heft-Nr. 641/2012 — "The Expedition of the Research Vessel "Maria S. Merian" to the South Atlantic in 2011 (MSM 19/2)", edited by Gabriele Uenzelmann-Neben